JOURNAL OF GEOPHYSICAL RESEARCH, VOL. 101, NO. C5, PAGES 12,001–12,016, MAY 15, 1996

Air-sea exchange of water vapor and sensible heat: The Humidity Exchange Over the Sea (HEXOS) results

J. DeCosmo,[1] K. B. Katsaros,[2] S. D. Smith,[3] R. J. Anderson,[3]
W. A. Oost,[4] K. Bumke,[5] and H. Chadwick [6]

Abstract. Surface layer fluxes of sensible heat and water vapor were measured from a fixed platform in the North Sea during the Humidity Exchange over the Sea (HEXOS) Main Experiment (HEXMAX). Eddy wind stress and other relevant atmospheric and oceanic parameters were measured simultaneously and are used to interpret the heat and water vapor flux results. One of the main goals of the HEXOS program was to find accurate empirical heat and water vapor flux parameterization formulas for high wind conditions over the sea. It had been postulated that breaking waves and sea spray, which dominate the air-sea interface at high wind speeds, would significantly affect the air-sea heat and water vapor exchange for wind speeds above 15 m/s. Water vapor flux has been measured at wind speeds up to 18 m/s, sufficient to test these predictions, and sensible heat flux was measured at wind speeds up to 23 m/s. Within experimental error, the HEXMAX data do not show significant variation of the flux exchange coefficients with wind speed, indicating that modification of the models is needed. Roughness lengths for heat and water vapor derived from these direct flux measurements are slightly lower in value but closely parallel the decreasing trend with increasing wind speed predicted by the surface renewal model of *Liu et al.* [1979], created for lower wind speed regimes, which does not include effects of wave breaking. This suggests that either wave breaking does not significantly affect the surface layer fluxes for the wind speed range in the HEXMAX data, or that a compensating negative feedback process is at work in the lower atmosphere. The implication of the feedback hypothesis is that the moisture gained in the lower atmosphere from evaporation of sea spray over rough seas may be largely offset by decreased vapor flux from the air-sea interface.

Introduction

The air-sea exchange of water vapor, heat, and momentum is important to many scales of atmospheric and oceanic motions. The latent heat flux is often the largest term in the heat balance of the upper ocean. Latent heat released when atmospheric water vapor condenses during cloud formation is important to synoptic- and climatic-scale atmospheric motions. However, sensible heat and water vapor fluxes have rarely been successfully measured in moderate to high wind conditions over the ocean [e.g., *Smith*, 1980, 1989; *Friehe and Schmidt*, 1976], and the underlying physics of these exchange processes over rough seas are not well understood [*Donelan*, 1990]. *Isemer et al.* [1989], examining air-sea flux parameterizations for the calculation of meridional oceanic heat transport [*Isemer and Hasse*, 1987], state that:

> Among six parameters which contribute mainly to the significance of air-sea energy fluxes [on a global scale] the transport coefficient C_E of latent heat flux is especially crucial: In spite of a large amount of experimental data its uncertainty is unacceptably high for calculations of climatological heat transports.

In light of the present focus of scientific effort on climate change and the global water cycle, and specifically on the modeling of large-scale air-sea heat exchange and its effects on climate, accurate determination of the water vapor exchange and its dependence on other parameters is of great importance.

The Humidity Exchange Over the Sea [HEXOS] program was designed to provide measurements of air-sea fluxes of water vapor and liquid water, primarily, under moderate to high wind speed conditions [*Katsaros et al.*, 1987; *Smith et al.*, 1989]. The program consisted of two field experiments, HEXPILOT [HEXOS pilot experiment] in 1984 and HEXMAX [HEXOS Main Experiment] in 1986, several wind/wave tunnel experiments [*Edson*, 1989; *Mestayer and Lefauconnier*, 1988; *Mestayer et al.*, 1990a,b], and modeling studies aimed at understanding air-sea heat and water exchange [*Edson*, 1989; *Rouault*, 1989; *Rouault et al.*, 1991; *Monahan et al.*, 1986; *Mestayer et al.*, 1990a,b]. This paper presents the measurements of water vapor and sensible heat fluxes above the sea surface collected by several of the participating groups during HEXMAX, and interprets these data in the context of relevant environmental parameters and the results of previous field work, modeling, and wind/wave tank studies.

Background

The Marine Surface Layer

In the atmospheric surface layer (the lowest tens of meters above the surface), fluxes of momentum, heat, and mass are

[1]Geophysics Program, University of Washington, Seattle.
[2]Department of Atmospheric Sciences, University of Washington, Seattle.
[3]Department of Fisheries and Oceans, Bedford Institute of Oceanography, Dartmouth, Nova Scotia, Canada.
[4]Ministry of Transport and Public Works, Royal Netherlands Meteorological Institute, De Bilt, the Netherlands.
[5]Institüt für Meereskunde and der Universitat Kiel, Kiel, Germany.
[6]U.K. Meteorological Office, Bracknell, Berkshire, England.

Paper number 95JC03796.
0148-0227/96/95JC-03796$09.00

assumed to be approximately constant, and the average values of horizontal wind speed, potential temperature, and water vapor density are expected to vary logarithmically with height above the surface for neutral density stratification [e.g, *Businger*, 1982]. Empirical formulas have been derived from data collected mainly over land [e.g., *Businger et al.*, 1971] to account for deviations in the profiles from purely logarithmic in the diabatic case where the density stratification of this layer is different from neutral. The integrated forms of the profile relations are as follows:

$$U(z) - U_s = \left(\frac{u_*}{k}\right)\left\{\ln\left(\frac{z}{z_o}\right) - \Psi_m\right\} \quad (1)$$

$$\Theta(z) - T_s = \left(\frac{t_*}{k}\right)\left\{\ln\left(\frac{z}{z_t}\right) - \Psi_t\right\} \quad (2)$$

$$Q(z) - Q_s = \left(\frac{q_*}{k}\right)\left\{\ln\left(\frac{z}{z_q}\right) - \Psi_q\right\} \quad (3)$$

$U(z)$, $\Theta(z)$, and $Q(z)$ are horizontal wind speed, potential temperature, and specific humidity evaluated at a height z. U_s, T_s, and Q_s are the horizontal wind speed, temperature, and specific humidity just above the surface (for a solid surface the surface speed will be zero, but this is not necessarily the case over a dynamic surface such as water), and u_*, t_*, and q_* are the friction velocity and scaling parameters for temperature and specific humidity in the atmospheric surface layer, respectively. The virtual origins of the profiles are the roughness lengths z_o, z_t and z_q, and k is the von Karman constant, here taken to be 0.4 [*Zhang et al.*, 1988]. Ψ_m, Ψ_t, and Ψ_q are the integrated forms of the functions of the lower level stability, $\zeta = z/L$, for wind speed, temperature, and water vapor; we have used the expressions for these functions recommended by *Dyer* [1974] in this analysis. L is the Monin-Obukhov length defined by

$$\frac{1}{L} = -\left(\frac{gk}{u_*^3}\right)\left[\frac{\langle tw\rangle}{(T+273.15)} + 0.61\langle qw\rangle\right] \quad (4)$$

where g is the acceleration due to gravity, t, w, and q are the fluctuation of temperature, vertical velocity, and humidity, respectively, and angle brackets represent a temporal average. The scaling parameters are related to the fluxes of momentum τ (or wind stress), sensible heat H, and water vapor flux E, through the following relations:

$$\tau = \rho u_*^2 \quad (5)$$

$$H = -\rho c_p u_* t_* \quad (6)$$

$$E = -\rho u_* q_* \quad (7)$$

where ρ is air density and c_p is heat capacity of air at constant pressure.

The bulk parameterization formulas for wind stress, sensible heat flux, and evaporation rate at the sea surface are

$$\tau = \rho C_D (U - U_s)^2 \quad (8)$$

$$H = \rho c_p C_H (U - U_s)(T_s - \Theta) \quad (9)$$

$$E = \rho C_E (U - U_s)(Q_s - Q) \quad (10)$$

U, U_s, T, T_s, Q, and Q_s are the horizontal wind speed, temperature and specific humidity at measurement height and at the surface, respectively. These formulas provide a practical method of estimating air-sea fluxes from average measurements of temperature, wind speed, and water vapor density if the value of the flux exchange coefficients are known. C_D, C_H, and C_E are the drag coefficient, and sensible heat and water vapor exchange coefficients (or Stanton and Dalton numbers, respectively) evaluated at measurement height, usually 10 m. The behavior of these coefficients over water surfaces has been studied in the laboratory and the field by many investigators (e.g., *Smith* [1980], *Liu et al.* [1979], *Geernaert et al.* [1986], *Smith* [1989], *Garratt and Hyson* [1975], *Kruspe* [1977] to name just a few), and has been modeled in terms of the surface roughnesses and Prandtl number (ratio of diffusivities of momentum and heat or mass) (e.g., *Liu et al.* [1979] and *Kitaigorodskii and Donelan* [1984], among many others). The effects of molecular constraints on the exchanges of momentum, sensible heat, and water vapor at an air-water interface have been studied in the laboratory and modeled by several investigators [e.g., *Owen and Thompson*, 1963; *Brutsaert*, 1975; *Deacon*, 1977; *Liu et al.*, 1979; *Kitaigorodskii*, 1984; *Kitaigorodskii and Donelan*, 1984]. In general these studies predict a weaker dependence of the Stanton and Dalton numbers on the roughness Reynolds number ($Rr = z_o u_* / \nu$ where ν is the viscosity of air) than that shown by the drag coefficient.

Measurements over oceans and lakes give an average value of the Dalton number for a neutrally stratified layer of 1.2×10^{-3} for low-level wind speeds from 4 to 14 m/s [*Smith*, 1989], with an average standard deviation of about 25%. With few exceptions (e.g., data collection in a surf zone by *Anderson and Smith* [1981], isotopic measurements in a wind/wave tunnel by *Merlivat* [1978]), no systematic dependence of the measured Dalton number adjusted to neutral stratification, C_{EN}, on environmental parameters has been demonstrated. *Launiainen* [1983], who included those two data sets in his summary, postulated that C_E follows about two-thirds the variations in C_D. Other theories have predicted a decrease in C_{EN} with wind speed [e.g., *Liu et al.*, 1979]. The average value of the sensible heat flux coefficient adjusted for neutral conditions, C_{HN}, tends to be slightly lower than C_{EN} (the Prandtl number is also smaller), with an average of 1.0×10^{-3} or slightly unstable conditions, and 0.8×10^{-3} for slightly stable conditions [*Smith*, 1980; *Large and Pond*, 1982; *Geernaert*, 1990). The difference between average values for different diabatic regimes indicates that the adjustment to neutral stratification typically performed on field data has been incomplete. Because of the large errors in individual eddy flux measurements which result from measurement error, approximations such as assumptions of steady state and homogeneous flow, and variability inherent in sampling a continuous process with finite samples of data [*Donelan*, 1990], there may be systematic variations of the flux exchange coefficients which have previously escaped notice. This, combined with the additional problems involved in carrying out these measurements in strong wind conditions leads to much doubt about the behavior of these coefficients, particularly above 14 m/s, where no direct field measurements have been reported.

Influence of Breaking Waves and Spray on Surface Fluxes

The air-sea energy and mass exchange process becomes more complicated when strong winds cause a high incidence of wave breaking. Whitecaps begin to appear on the ocean surface at wind speeds as low as 3 m/s; actively breaking waves cover a significant fraction (>1%) of the ocean surface at wind speeds of about 10 m/s [*Monahan and O'Muircheartaigh*, 1980]. Whitecap

coverage increases at a rate approximately proportional to the cube of the surface layer wind speed [*Spillane et al.*, 1986; *Monahan et al.*, 1983b]. Breaking waves alter the surface roughness characteristics of the ocean [e.g., *Donelan*, 1990] and produce sea spray droplets. Thus, at wind speeds higher than about 6 m/s, the air-sea water vapor flux is a combination of the evaporation of liquid water from the sea surface and the evaporation from sea spray droplets ejected into the atmosphere in the vicinity of breaking waves.

If all of the vapor flux E originates at the sea surface, the associated latent heat is lost by the sea and gained by the atmosphere. Thus the air-sea latent heat flux is typically calculated by multiplying E (equation (10)) by L_ω, the latent heat of vaporization. If a portion of the vapor flux measured at a few meters' height above the surface has resulted from evaporation of spray droplets in the layers below, then a corresponding portion of the latent heat supplied to the atmosphere above the droplet layer derives from the air below it. Ejection and subsequent evaporation of spray droplets do not directly affect the heat budget of the sea. However, feedback processes may be initiated: cooling of the lowest portion of the atmosphere by evaporating droplets will stimulate an increased sensible heat flux from the sea surface, while moistening of the near-surface layer will inhibit the surface evaporation rate [*Edson*, 1989; *Katsaros and DeCosmo*, 1990; *Donelan*, 1990]. The evaporation of spray droplets would perturb both the temperature and humidity profiles if the amount of water added to the lower atmosphere were significant. This could result in vertical variations in the turbulent fluxes of heat and moisture within the so-called "constant flux" layer.

The modeling study by *Stramska* [1987], and later the HEXOS simulation tunnel modeling studies described in the next section, probe some of these issues. *Smith* [1990] presents a simple approach to the parameterization of these effects in the context of the surface layer profile relations. This latter work suggests that, from the viewpoint of a measurement height above a droplet evaporation layer, the effect of droplet evaporation would be to modify the apparent boundary conditions.

Since the measurements reported here were collected at one height, several meters above the air-sea interface, it is not possible to separate the potential droplet and interfacial contributions to the measured fluxes. Therefore the net sensible heat and vapor fluxes at measurement height will be reported in the results section, and note that the latent heat lost by the ocean may not be equal to $L_\omega E$.

Early laboratory studies. *Wang and Street* [1978] carried out experiments in the Stanford Wind, Water-Wave Research Facility to estimate the contribution of evaporating spray on surface fluxes of heat and water vapor. They calculated the flux of water vapor and heat due to the evaporating droplets, and the total energy transfer above the droplet boundary layer from the measurements of temperature, humidity, and droplet concentration profiles. The spray was produced by breaking of wind waves, and the droplet number concentration spectra compared well with most other field and laboratory measurements [*Wang and Street*, 1978]. They found that the energy transfer from droplets does increase as the wind speed increases, but the contribution of the droplets to the total energy flux was always less than 2%. An increase in total energy transfer with increasing wind speed was observed, and this increase correlated very well with root mean square wave amplitude, leading them to conclude that the increase in energy transfer was closely related to surface wave conditions. The authors cautioned against simple extrapolation of these results to field conditions due to the large difference in the height of the droplet boundary layer for the two situations. Taking this into account by using data from *Preobrazhenskii* [1973], the authors estimated that evaporation from droplets in the field would be about twice what they observed in the laboratory, and they concluded that since the total energy transfer in the field is lower than for the laboratory conditions, the ratio of droplet contribution to total water vapor or heat flux may be greater for field conditions. However, due to development of saturation conditions in the lower boundary layer and the strong interactions between the low-level temperature and humidity fields, a prediction cannot be made on the basis of laboratory results. The general conclusion of this work was that field measurements were badly needed.

Modeling studies. Numerical models have also been used to make predictions about the effect of sea spray on the air-sea mass and energy exchange. Some of the original inspiration for the HEXOS program came from a pioneering article by *Ling and Kao* [1976]. In that and subsequent papers from the same group [*Ling et al.*, 1978, 1980], the authors addressed the role of sea spray in the modification of the lower atmosphere. *Ling and Kao* [1976] solved a system of three coupled differential equations in the dependent variables: temperature, humidity, and spray droplet concentration. The three variables are coupled, since evaporating spray both cools and humidifies the atmosphere. The equations were closed by assuming K-theory eddy diffusivity. Results from this steady state model predicted that the moisture and heat fluxes would be dominated by sea spray contributions at high wind speeds. For a low-level wind of 20 m/s, and a sea-air temperature difference of 5°C, the modeled sensible and latent heat fluxes due to evaporating spray droplets were approximately 3 times the values estimated from the bulk formulas for surface evaporation and heat flux. These results, of course, were sensitive to the effective droplet size and number concentration used for their calculation, which were quite large in comparison with those derived from measured droplet spectra [e.g., *Fairall et al.*, 1983]. A later version of this model [*Ling et al.*, 1980] included several drop size categories and explicitly accounted for the gravitational fallout of the larger drops. Predictions about the effect on vapor and heat fluxes were similar, but more modest than in the earlier version. Some field measurements were compared to model predictions, but these results were inconclusive.

The approach of *Ling and Kao* [1976] and *Ling et al.* [1980] was extended to include time dependence and more realistic drop-size categories by *Stramska* [1987], who employed *Monahan et al.*'s [1983b] formula for surface production of aerosol flux (droplets with dry radius <15 μm), and drop size distributions of *Preobrazhenskii* [1973] for large droplets (dry radius >15 μm). She found that evaporation of the large droplets may significantly perturb the water vapor and temperature profiles very close to the sea surface for wind speeds above about 15 m/s. These calculations showed that at wind speeds of 15-25 m/s, evaporation of the large droplets may increase the relative humidity by 10% in the lower surface layer, and decrease the temperature by as much as 2°C. These effects indicate that direct interfacial moisture and heat exchange may be affected by evaporation of spray at some distance above the interface. No attempt was made by Stramska to estimate the effect of the changed profiles on net surface fluxes.

Another modeling study by *Bortkovskii* [1987] predicted that the contribution of sea spray to the fluxes of heat and water vapor during high wind conditions would be large. This budget model considered the heat and mass transfer from a drop which is

ejected at the sea surface, spends some time in the atmosphere near the surface, then reenters the sea. The differential mass and heat exchange for a drop, multiplied by the probability density of drop generation, and integrated over droplet radius and along the profile of a breaking wave, yielded an estimate of the fluxes due to one whitecap. Formulas for drop-size distribution, distribution of spray along the profile of a breaking wave, and the areal coverage of whitecaps, were all assumed. The coefficients of heat and vapor exchange were considered to be composed of two parts, one due to the turbulent fluxes at the air-sea interface, and one due to the contribution from evaporating spray. The empirical formulas for whitecap coverage and drop size distribution used in this study were quite different from those used by *Stramska* [1987] or *Ling and Kao* [1976], and the calculations are very sensitive to these quantities. The turbulent parts of the exchange coefficients for sensible heat and water vapor were assumed to be constant, equal to each other, and at 15 m/s to have a value of 1.35×10^{-3}. For wind speeds higher than 15 m/s, the exchange coefficients were predicted to increase dramatically due to the evaporation of droplets, reaching values of approximately 3.5×10^{-3} at 30 m/s.

Simulation experiments. In 1984-1988, HEXOS researchers carried out the HEXIST (HEXOS Experiments in the Simulation Tunnel) and CLUSE (Couche Limite Unidimensionnelle Stationnaire d'Embruns; one-dimensional stationary bubble boundary layer) experiments to investigate the effects of bubble-produced droplets on the turbulent exchange of heat and moisture above an air-water interface [*Smith et al.*, 1989; *Mestayer et al.*, 1990a]. The experiments took place in the wind/wave simulation tunnel at Institut Méchanique Statistique de la Turbulence (IMST) in Luminy, France, and in the wave tank at the University of Connecticut [*Smith et al.*, 1989]. The first series of experiments focused on the effects produced by a simulated whitecap located various distances upstream of the measuring sensors. Profiles of droplet concentration, temperature, humidity, and heat fluxes were collected for various ambient conditions. A Lagrangian model of the behavior of evaporating droplets generated by a point source [*Edson*, 1989] was successful in reproducing the droplet concentration profiles measured in the tunnel.

In the 1988 CLUSE experiment the single simulated whitecap was replaced by a homogeneous and random distribution of bubble patches along the entire 30-m length of the simulation tank. A one-dimensional ensemble-average Eulerian model was developed in connection with the CLUSE simulations to study the interactions between turbulent scalar fields and the spray droplets [*Rouault*, 1989]. Results from the CLUSE tunnel experiment show that droplet evaporation increased the mean absolute humidity, particularly near the interface, while the measured turbulent latent heat flux decreased at all points in the boundary layer, compared to the control case with no droplets present [*Mestayer et al.*, 1990a]. These measurements provide some evidence for the negative feedback process discussed above. As droplets evaporate, the lower boundary layer becomes moistened, and the latent heat flux from the air-water interface is reduced owing to decreased near-surface water vapor gradient. Again, it is difficult to extrapolate the results of simulation tank measurements to model or field situations; a constant flux layer does not exist in the tunnel, with or without the evaporating droplets, indicating that horizontal advection in the upper tunnel layer is not negligible [*Rouault et al.*, 1991]. The CLUSE numerical model results also show evidence of negative feedback. However, the authors caution that the production of vapor from evaporating droplets may increase faster with increasing wind speed than the concomitant reduction in surface vapor flux. The consequence is that the influence of droplets on the net vapor and heat fluxes could be significant at very high wind speeds [*Mestayer et al.*, 1990a].

A recent modeling study by *Andreas* [1992] also concludes that at high wind speeds the effect of droplet evaporation should be significant. This model is based on calculations of the length of time that sea spray droplets reside in the lower atmosphere and the moisture and heat they exchange with their environment during this residence time. Unlike previous modeling studies, this model calculates the influence of spume droplets using a semi-empirical generation function. The predicted effect on the moisture flux for a 20 m/s wind is significant, and about 5 times the predicted effect on the sensible heat flux. The author does not include the modifying effect on the profiles of temperature and humidity such as were observed in the CLUSE wind/wave tunnel experiments [*Mestayeret al.*, 1990a]. He leaves the evaporation from the air-sea interface unchanged, which is not likely to be a realistic assumption if the evaporation of droplets is as large a fraction of the flux as he suggests (*Katsaros and de Leeuw* [1994]; see also the response by *Andreas* [1994]). A common conclusion of all attempts to model evaporation from the sea in spray conditions is that a more accurate source function is required.

Data Collection and Analysis

The HEXMAX Experiment

The HEXOS Main Experiment, HEXMAX, took place from October 6 to November 28, 1986, near the Dutch coast on and in the vicinity of the Dutch Research Platform Noordwijk (MPN) [*Smith et al.*, 1989]. Participating groups on MPN collected comprehensive measurements of fluxes of water vapor, heat and momentum, turbulence statistics, sea state, whitecap coverage, radiation and aerosol concentration, and composition. Surface flux measurements were also made from the research vessel the RRS *Frederick Russell,* from a tripod-based mast operated by the Institut für Meereskunde, Universitat Kiel (IfM) located between MPN and the nearby shore, and from the British Meteorological Office (BMO) C-130 Hercules instrumented aircraft. This paper presents the analysis and interpretation of the water vapor and sensible heat flux data collected on MPN, from the tripod and from the aircraft during HEXMAX.

Favorable weather conditions and reliable performance of the measurement sensors and recording systems on MPN resulted in the collection of well over 300 hours of data in the wind speed range of 6–27 m/s. Fewer hours of data were recorded at the IfM tower due to its unfortunate destruction during the storm of October 19–20. The C-130 aircraft flew five times during HEXMAX. Weather was characterized by the passage of a series of low-pressure systems, moving from southwest to northeast. Winds in the prefrontal regions were generally from the south, veering to the west following the passage of a frontal boundary, where sustained periods of strong winds were accompanied by a wide range of relative humidities (50% to 100%). Westerly winds dominate the data set, with an average speed of 12.6 m/s at 10-m height.

Method of Flux Calculation

Surface layer fluxes reported in this paper were measured with the eddy correlation method by several participating groups

operating from the MPN platform, the BMO aircraft, and the IfM mast. To directly measure the eddy fluxes of momentum (τ), sensible heat (H), and water vapor (E) in the atmospheric surface layer, fluctuations of horizontal wind (u), temperature (t), and specific humidity or water vapor mixing ratio (q) are correlated with vertical wind fluctuations (w) [e.g., *Busch*, 1973] for an appropriate averaging time, indicated by angle brackets. Alternatively, the fluctuations of water vapor density (absolute humidity) $\rho_v = \rho q$ may be used:

$$\tau = -\langle \rho uw \rangle \tag{11}$$

$$H = c_p \langle \rho tw \rangle \tag{12}$$

$$E = \langle \rho qw \rangle = \langle \rho_v w \rangle \tag{13}$$

Fluctuations in the air density ρ make a negligible contribution to the fluxes and ρ can be taken outside the angle brackets, $H = \rho c_p \langle tw \rangle$ etc., so the fluxes can be calculated from time series measurements of the fluctuating quantities w, u, t, and q or ρ_v. The optimum averaging period for flux calculations depends on the height of the measurements, the mean wind speed, and the steadiness of the flow. Most of the flux estimates calculated from the MPN and tower data are based on averaging periods between 40 and 60 min. In a few cases of highly variable conditions and strong winds, shorter periods were used. The measurements taken from the C-130 aircraft represent a spatial average over 25 km.

Flux estimates were also obtained with the inertial dissipation method from the MPN platform and from the RRS *Frederick Russell*. Descriptions of the systems used and comparisons between the fluxes obtained by the eddy correlation and inertial dissipation methods are reported by *Fairall et al.* [1990], *Edson et al.* [1991] and *Smith et al.* [1992].

Data collected from MPN. The fast-responding flux measurement sensors were located at the tip of a boom (Figure 1) extending 18 m west from MPN at an adjustable height between 6 and 10 m above mean sea level. Despite the strong winds experienced throughout most of the data collection period, vibration of the boom was minimal, and it maintained a horizontal level to within ±0.2°. Average values of atmospheric temperature and humidity at 17 m above mean sea level, sea surface temperature, and wave height were recorded by the MPN standard instruments.

The presence of sea-salt aerosol in the marine environment makes the measurement of sensible heat and water vapor fluxes technically difficult to carry out in moderate conditions, and in the past has defeated all attempts at high wind speeds. Liquid water present on the windows of a Lyman α humidiometer, a dew point sensor, or a temperature sensor will temporarily invalidate

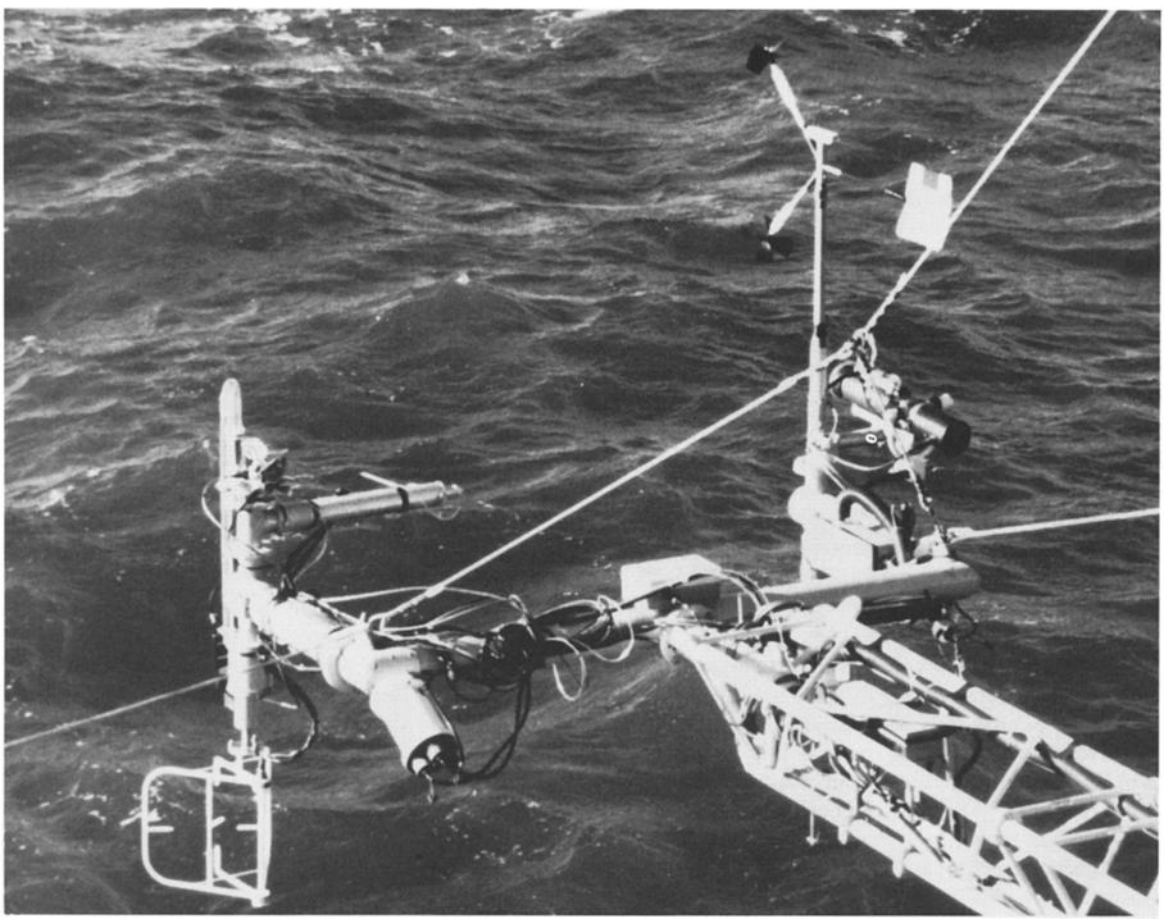

Figure 1. Sensors on the boom during HEXMAX. At the right (north) end of the crossbar, the UW K-Gill anemometer is above the boom and the spray flinger aspirator is beside it on the right, with a thermocouple psychrometer and Lyman α humidiometer inside. The KNMI sonic and pressure anemometers are below the boom on the left and right sides, respectively. The BIO refinery aspirator is above the boom at the left, with the inlet extending down toward the sonic anemometer.

the measurements. Temperature sensors used for atmospheric turbulence measurements must be exposed to the turbulent airstream to respond rapidly to the fluctuating temperature for flux estimates. Once small sea-salt particles are deposited on these sensors, water deliquesces or evaporates as air parcels of high or low relative humidity pass by. This results in a signal contaminated by the rate of change of humidity, which is sometimes detected by the presence of "cold spikes" in the time series of fluctuating temperature [*Schmitt et al.*, 1978; *Katsaros et al.*, 1994; *Fairall et al.*, 1979]. Though this problem has been noted in many previous investigations [e.g., *Friehe and Schmitt*, 1976; *Davidson et al.*, 1978], it continues to plague marine boundary layer scientists.

To make reliable measurements of sensible heat and water vapor fluxes in stormy marine conditions, it is therefore necessary to protect temperature and humidity sensors from contact with airborne sea-salt aerosols or to replace and clean them very frequently. Protective housings intended to remove aerosols and to interfere minimally with the measurement of temperature and humidity were developed by the Royal Netherlands Meteorological Institute (KNMI), the Bedford Institute of Oceanography (BIO) and the University of Washington (UW) groups [*Katsaros et al*, 1994]; of these the "spray flinger" housing employed by the University of Washington had the best overall performance.

The UW spray flinger was designed to minimize flow modification on scales important to the eddy correlation calculations employing data from temperature and humidity sensors inside the housing. The spray flinger is a 60-cm-long tube, 10 cm in diameter, with a rotating filter screen and fan on the upwind end, and an exit fan and the motor at the downwind end. The filter is a single layer of nylon stocking, which is highly nonabsorbing, supported by a wire mesh. Particles and droplets are intercepted by the rotating filter and flung aside, out of the airstream entering the tube. The rotation rate of the filter is 625 rpm. Inspection of the filter revealed that this rate of rotation prevented buildup of water or salt. The nylon filter was replaced at weekly intervals. Since the wind speed inside the spray flinger is dependent on ambient winds, a time lag is introduced for the temperature and humidity measurements which is greatest at low ambient wind speeds. Field tests showed that the spray flinger interfered minimally with turbulent measurements up to about 3 Hz, and removed more than 95% of droplets with diameters 5 μm and larger from the sample airstream. Details of these tests are found in the work by *Katsaros et al.* [1994].

UW sensors and analysis procedure. The fast-responding sensors used by UW for eddy correlation flux measurements at the boom tip included a K-Gill twin propeller-vane anemometer [*Ataktürk and Katsaros*, 1989] for mean and fluctuating horizontal and vertical wind speeds, a set of miniature wet- and dry-bulb thermocouples for mean and turbulent wet- and dry-bulb temperatures and atmospheric humidity, and a Lyman α humidiometer for fluctuating water vapor density. The K-Gill was mounted on the north end of the boom crossbar, 1.1 m above the boom level (Figure 1). The temperature and humidity sensors, housed in the spray flinger, were mounted beside the K-Gill, 0.6 m above the boom level. Data from these sensors were digitized using a frequency shift keying (FSK) unit and stored serially on tape by an analog Hewlett Packard (3968A) tape recorder. The sampling rate for each channel was 27.27 Hz, and the signals were low-pass filtered at 7 Hz. Eddy fluxes were calculated by correlating the instantaneous vertical wind from the K-Gill with the K-Gill fluctuating horizontal wind, instantaneous temperature from the dry thermocouple, and fluctuating water vapor density from both the Lyman α humidity signal and from the thermocouple psychrometer. The K-Gill winds were rotated into coordinates aligned with the mean wind, and linear trends were removed from all channels. About 197 hours of data divided into run lengths of mostly 40-60 min were analyzed.

The Lyman α humidiometer, a model AIR-LA-1, has a time response of 2 ms and measures variations in water vapor density to high precision (0.2% of value). This sensor must be calibrated in situ because the output of its source tube and the efficiency of its detector vary over time and with environmental conditions. This was accomplished by calibrating the mean absolute humidity each hour against that given by a slow-response psychrometer.

The miniature psychrometer used for turbulence measurements consisted of two type E chromel-constantan fast-responding thermocouple sensors located in the aspirator, 10 cm ahead of the Lyman α. The wet sensor was a 25-μm or 50-μm diameter thermocouple covered with cotton; a reservoir and plumbing system provided continual moistening of the wick. The dry thermocouples (both 25- and 50-μm diameter thermocouples were used as dry sensors) had a time response of less than 0.036 s (which was the sampling rate) for wind speeds above 5 m/s [*Shaw and Tillman*, 1980].

Dry- and wet-bulb temperatures were combined to obtain instantaneous values of specific humidity. The wet thermocouple has greater thermal inertia, resulting in a frequency response well below that of the dry thermocouple. In unstable conditions, the water vapor flux is underestimated unless the time responses of the two thermocouples are matched [*Tsukamoto*, 1986]. If the time constants of both sensors are known, a partial correction may be applied to the time series of the slower sensor (here the wet bulb) on the basis of the assumption that it acts as a simple low-pass filter [*Shaw and Tillman*, 1980].

We determined the time constant of the wet-bulb sensor by comparing the power spectrum of the wet thermocouple with a "simulated" wet-bulb spectrum calculated from concurrent time series from the faster-responding Lyman α humidity sensor and the dry-bulb thermocouple. For fluctuations of frequency less than about 4 Hz, both the Lyman α and the 25-μm dry-bulb thermocouple may be assumed to have a perfect time response. Figure 2a shows a sharp rolloff of the uncorrected wet-bulb power spectrum above 0.1 Hz, as compared to the simulated wet-bulb spectrum. Figure 2b shows the water vapor density spectrum using the adjusted wet-bulb signal (time constant of 0.758 s in this example), compared to the water vapor density power spectrum derived from the Lyman α signal. An upturned tail of the psychrometer-derived water vapor density spectrum above 1.5 Hz indicates high-frequency noise in the time series that has been amplified by the correction procedure. However, as may be seen from the wq cospectrum illustrated in Figure 2c, this noise is uncorrelated with vertical velocity and, consequently, does not affect the calculation of water vapor flux. The wq covariance calculated with the corrected psychrometer data is still, on average, about 8% lower than the covariance calculated with the Lyman α signal for simultaneously recorded data. Table 1 gives some examples of the sign and magnitude of the error involved in using unmatched thermocouples without the above correction, and the error remaining after the correction is applied. The time response of the wet-bulb sensor varied between 0.2 and 1.0 s [*DeCosmo*, 1991].

Though this time response leads to a relatively low cutoff frequency, recent work by *Behrens* [1993], indicates that for HEXMAX-like conditions a cutoff frequency of 1 Hz is sufficient

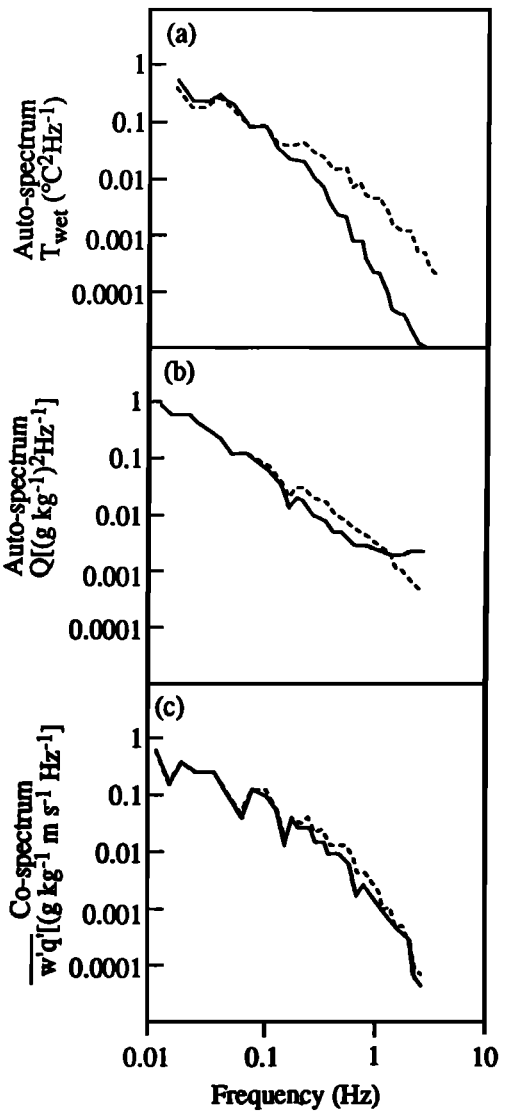

Figure 2. (a) Spectra of wet-bulb temperature (T_{wet}), measured (solid line) and simulated (dashed line); see text. (b) Spectrum of water vapor density using the wet-bulb signal adjusted with a time constant of 0.756 s (solid line) and the Lyman α humidiometer (dashed line). (c) Cospectrum of vertical velocity and water vapor density for the corrected psychrometer (solid line) and the Lyman α (dashed line).

for obtaining 98% of the temperature or humidity covariance. Excellent agreement between covariances calculated using simultaneously recorded signals from faster and slower responding humidity sensors (i.e., those inside and just outside of the BIO aspirator [see *Katsaros et al.*, 1994]) was also obtained during HEXMAX, lending further credibility to these flux estimates.

The lag in response for the sensors mounted inside the spray flinger was dependent on the mean wind speed and was less than one sample (0.036 s) at all times for the thermocouple psychrometer, was one to two samples for the Lyman α at wind speeds below 8.5 m/s, and less than one sample for the Lyman α for higher mean winds. Though most of the airborne salt particles were removed from the air entering the housing, some accumulation of salt on the thermocouples was noted occasionally during the data collection period. The temperature sensors were replaced and cleaned as frequently as possible, and data were carefully examined for evidence of contamination.

Two slow-response platinum resistance thermometers, one wet-bulb platinum resistance thermometer, and one LiCl dew point hygrometer were mounted at 17 m above mean sea level on the boom deck to monitor mean temperature and humidity. The wet-bulb thermometer was our modification of an ordinary resistance thermometer. All sensors were housed in controlled airflow assemblies and were protected from direct sunlight by radiation shields (all from the R.M. Young Co.). Data from these sensors were recorded continuously during the 6-week experimental period. The time series of 10-min averages provided reliable values of mean temperature and humidity during HEXMAX for use in field calibrations of the turbulence sensors on the boom and in the bulk parameterization formulas [*Katsaros et al.*, 1994].

BIO sensors and analysis procedure. The BIO eddy flux temperature and humidity sensors were mounted below the south end of the boom, near the KNMI sonic anemometer, approximately 0.75 m below the boom's center, typically at 6 m above the mean sea level. These sensors included two Lyman α humidiometers, one shielded from marine aerosols in a protective housing described below, a microbead thermistor, and a miniature glass-coated thermistor. Time series of water vapor density from the Lyman α sensors and temperature obtained from fast responding thermistors were correlated with the time series of instantaneous vertical velocity obtained from the KNMI sonic anemometer to obtain the eddy fluxes of water vapor and sensible heat. The BIO data were low-pass filtered at 8 Hz and logged at 16 Hz in serial digital format for 45-min run lengths. The sonic anemometer data were rotated into coordinates aligned with the indicated mean wind, and linear trends were removed from all channels. Spectra, cospectra, and statistical properties were also computed from the time series. Approximately 42 hours of data have been fully analyzed.

BIO operated two Electromagnetic Research Corporation (ERC) Lyman α ultraviolet absorption humidiometers (model BLR) for measurements of water vapor fluctuations during

Table 1. Examples of Compensating for Wet-Bulb Response Time in Calculating Eddy Flux of Water Vapor

Mean Wind, m/s	$T_{sea}-T_{air}$, °C	Relative Humidity, %	Response Time, s	Water Vapor Flux, W / m²		Percent Change
				Uncorrected	Corrected	
15.5	4.0	61	0.330	265	286	+ 7
12.8	3.0	74	0.300	158	184	+ 14
12.7	3.4	57	0.300	186	204	+ 9
8.1	0.7	66	0.350	79	98	+ 19
8.9	0.8	63	0.477	75	92	+ 19
10.5	-1.5	88	0.590	16	12	- 33
10.3	1.4	80	0.605	91	109	+ 16

HEXMAX. One was mounted inside a "refinery" aspirator designed to remove liquid water from the sampling path [*Katsaros et al.*, 1994]. The other, exposed to the ambient airstream, was deployed only in the absence of rain, fog, and sea spray. Two different aspirators were used during the experiment, called "large" and "small"; one had a larger and more powerful suction fan than the other, but they were otherwise identical. Penalties inherent in this method of sensor protection are a lag in response, while the air travels from the inlet to the sensing volume and an attenuation of higher-frequency spectral components by mixing as the air travels through the tubing. Comparison between humidity spectra obtained from a Lyman α exposed directly to the airstream and spectra obtained from the sensor housed in the refinery showed the lag time to be 0.38 s for the small aspirator and 0.25 s for the large aspirator, and a loss of about 5% of the vapor flux to be due to mixing inside the tubing. The time series of water vapor density were shifted according to the appropriate lag time before eddy fluxes were calculated. The Lyman α sensors were recalibrated after HEXMAX in the humidity calibration facility of the Canada Centre for Inland Waters. The aspirated sensor judged to be the most reliable was compared as a secondary standard to the Lyman α sensors operated by UW and KNMI during HEXMAX.

A microbead thermistor (Victory Engineering Co. model E41A401) and a miniature glass-enclosed thermistor (Thermometrics, Fastip series FP07) were installed to measure mean air temperatures and high-frequency temperature fluctuations. According to manufacturer's specifications, both sensors have similar response times, but comparison showed the Fastip had complex spectral rolloff at the higher frequencies [*Katsaros et al.*, 1994]. These thermistors were exposed directly to the airstream but were shielded from solar radiation by small caps.

HEXIST inertial-dissipation packages. HEXIST participants from Pennsylvania State University, Risφ National Laboratory (Denmark), and Institut de Mécanique Statistique de la Turbulence installed two sets of sensors to measure spectra of velocity, temperature, and humidity, one on the boom and the other on a mast at the western edge of the platform in a region of considerable flow distortion, 7 m above the heli-deck and 26 m above sea level. Eddy fluxes computed from the package on the boom used the winds from the KNMI anemometer. These data have been used to compare dissipation and eddy correlation wind stress and sensible and latent heat flux, and to investigate the influence of flow distortion [*Fairall et al.*, 1990; *Edson et al.*, 1991].

KNMI sensors. KNMI operated two anemometers on the boom during HEXMAX, a Kaijo-Denki sonic anemometer on the south end of the boom tip and a pressure anemometer [*Oost*, 1983; *Oost et al.*, 1991] on the north end of the boom tip. Both anemometers provided measurements of instantaneous vertical and horizontal wind speed which have been used in the analysis of wind stress [*Smith et al.*, 1992] and the KNMI sonic anemometer data were used in the computation of eddy fluxes of water vapor and sensible heat by the BIO and HEXIST groups. A Lyman α humidiometer in a "vortex" aspirator gave good data part of the time [*Katsaros et al.*, 1994] but did not yield as large a set of humidity flux data as the UW and BIO sensors.

Flow Distortion Corrections

Mean values of temperature and water vapor density were obtained on MPN from the platinum resistance psychrometer described by *Katsaros et al.* [1994]. Mean horizontal wind was derived from the KNMI sonic or the K-Gill anemometer on MPN or from the propeller-vane anemometer on the IfM tower. Mean winds measured from the boom on MPN were adjusted to remove the influence of flow distortion by the MPN structure according to the results of the wind tunnel study by *Wills* [1984]. A small local distortion of the flow around the boom tip and surrounding sensors was also noted during HEXMAX. The "tilt" correction, aligning coordinates along the mean wind direction, was applied at all sensor positions. Details of the wind analyses are reported by *Smith et al.* [1992]. Indications based on *Wills'* [1984] tunnel measurements and theoretical results of *Wyngaard* [1981, 1988] are that flow distortion errors in scalar (heat and moisture) fluxes go as the error in vertical wind variance, and this error is expected to be much less than 5% for the HEXMAX instrument configuration on the boom [*DeCosmo*, 1991]. The helideck sensors amply illustrate the effect at such a location on eddy correlation measurements, while dissipation estimates of the turbulent fluxes were less affected [*Edson et al.*, 1991].

Data Collected From the IfM Tower

The IfM tower is a bottom-mounted tripod with a fixed instrument support at 8-m height above mean sea level. It was floated to a site with a water depth of 15 m between the MPN and the nearby shore at 52°15.33'N and 4°20.07'E. Data were telemetered to a shore station at Noordwijk. Measurements were collected from the tower for 9 days (October 10-19, 1986). On October 19 the tower was destroyed in a storm when wind gusts reached 35 m/s at measurement level. Twenty hours of observations, with winds of 4-10 m/s at measurement level coming from the seaward direction, were collected and analyzed.

The mast of the Kiel tripod, designed for minimal flow distortion, was instrumented with standard sensors for mean quantities of wind speed and direction, dry and wet air temperatures, water temperature, and incoming solar radiation. A three-dimensional propeller system and a fast psychrometer [see *Katsaros et al.*, 1994] both mounted on a wind vane, were used for calculation of turbulent fluxes.

The psychrometer consisted of type E dry- and wet-bulb thermocouples of 100- and 200-μm diameters, respectively. The cotton wick that fed the wet-bulb was wetted with distilled water by a peristaltic pump which provided continuous slow flushing of the wick. Correction for attenuation of propeller response at high frequencies (distance constant of 2.1 m) and for different time response of the dry- and wet-bulb thermocouples (0.15 and 0.40 s, respectively) were performed on the data. A slight dependence of thermocouple response time on mean wind speed was noted in the data but was not important for the range of wind speeds recorded. Sensible heat fluxes measured at the IfM mast, judged to be less reliable than the vapor flux results, will not be reported here.

Data Collected From the BMO Aircraft

Five flights were completed by the BMO C-130 Hercules research aircraft [*Nicholls*, 1978] during the HEXMAX experimental period. High-frequency measurements of the three wind components, air temperature and humidity, aerosol spectra, and radiative sea surface temperature were collected. Eddy fluxes of momentum, heat, and moisture were calculated on each run after linear detrending on the time series.

The flight pattern followed during all five flights is shown in Figure 3. Runs of approximately 25 km in length were completed along legs CD and GH, parallel to the coastline, at three heights: 30 m, 150 m, and 300 m. The flight leg AB, called the intercomparison leg, was oriented along wind as determined from

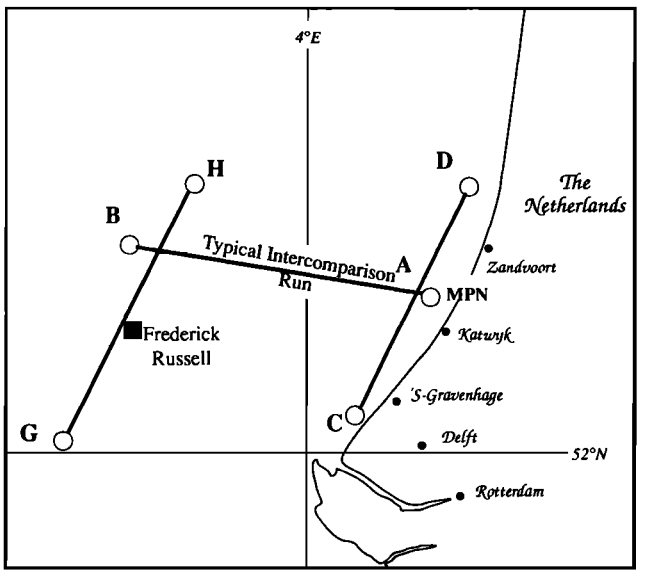

Figure 3. The flight pattern of the BMO aircraft during HEXMAX.

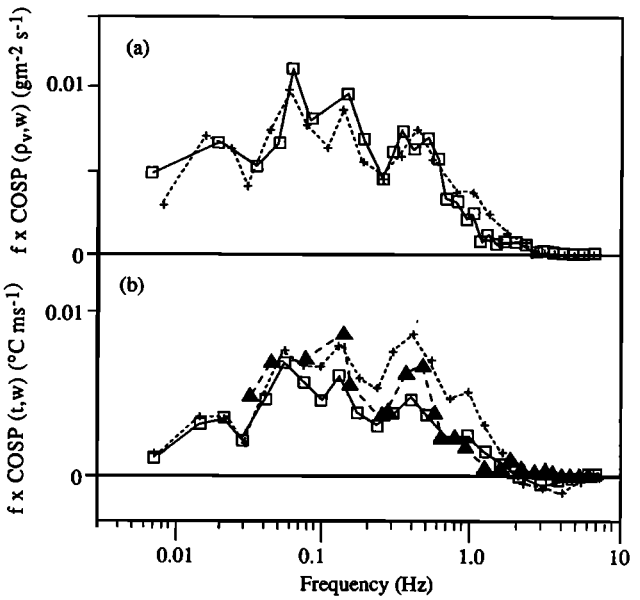

Figure 4. (a) Frequency times cospectrum of vertical wind and water vapor density from independent Lyman α measurements by the UW (crosses) and BIO (squares) sensors for a 45-min data run starting at 1308 UT on November 20, 1986. The area under the cospectrum is proportional to the water vapor flux. (b) Frequency times cospectrum of vertical wind and temperature measured by UW thermocouple (triangles), BIO microbead (crosses) and Fastip (squares) for the same data run.

the aircraft navigator winds between legs CD and GH, only at the lowest height. Some indication of the vertical structure of the atmosphere was obtained by profiling through the depth of the boundary layer at the beginning and end of each flight. Data from two of the five flights will be reported here.

Results

In the "constant flux" atmospheric surface layer the measured sensible heat and water vapor fluxes are usually assumed to be no more than 10% different from their values at the air-sea interface [e.g., *Fleagle and Businger,* 1980]. As discussed earlier, in the presence of evaporating (or growing) water droplets in the lower atmospheric boundary layer, the turbulent fluxes at heights above the surface may be significantly different from their values at the air-sea interface. Here, we report the net fluxes as measured at 6-8 m above mean sea level.

The measured fluxes and mean parameters obtained during HEXMAX were substituted into equations (9) and (10) to obtain values for the turbulent exchange coefficients for sensible heat and water vapor for comparison with predictions and results from previous studies. These coefficients will be discussed extensively in the next few sections.

Water Vapor Flux

The water vapor flux results of all participating groups operating on MPN and the IfM tower are in very good agreement. The effective latent heat flux was found to dominate the heat budget at the air-sea interface during most of the conditions encountered during HEXMAX in the autumn over the North Sea [*Taylor et al.,* 1991]; typically, the latent heat fluxes were of the order of hundreds of W/m^2, while the sensible heat and net radiative fluxes were of the order of tens of W/m^2. The effect of sea spray on the water vapor flux is not easily discernible from the water vapor flux measurements.

Samples of *wq* cospectra are given in Figure 4 from the UW and BIO sensor arrays for a simultaneous run during HEXMAX. Figure 5 shows a comparison of the water vapor flux calculated from simultaneous measurements carried out independently by BIO and UW during HEXMAX.

Figure 6a shows C_{EN} versus U_{10N} derived from data collected by the UW and BIO groups. Subdividing the data into blocks by relative humidity does not show any significant deviations from this plot.

To eliminate the complicated conditions of rain and high humidity, only data with no rain and relative humidity < 80% have been plotted. In addition, BIO data were selected by deleting runs if (1) rain occurred during or just prior to the data run, (2) the sonic anemometer probe was aimed more than 15° off the mean wind direction, possibly causing flow distortion by the probe, (3) contamination of the Lyman α tube faces was indicated by large overestimation (by a factor of ≥2) in the indicated mean humidity or (4) $|\rho_s - \rho_v| < 1 g/m^3$. There remain

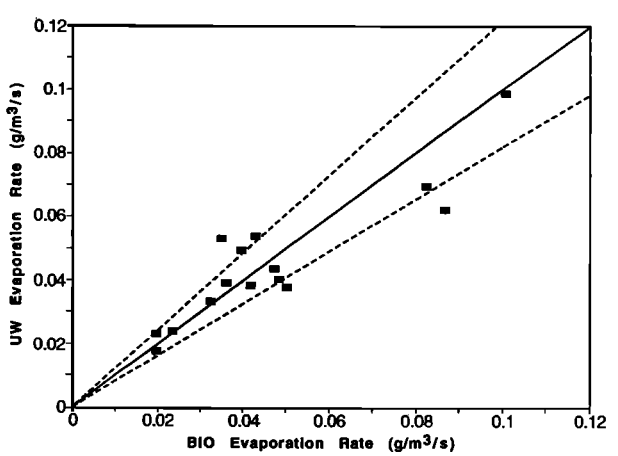

Figure 5. Comparison of water vapor fluxes measured independently by UW and BIO sensors during same time intervals. Most of the points lie within dashed lines $Y = 1.24X$, $X/1.24$, indicating estimated experimental error.

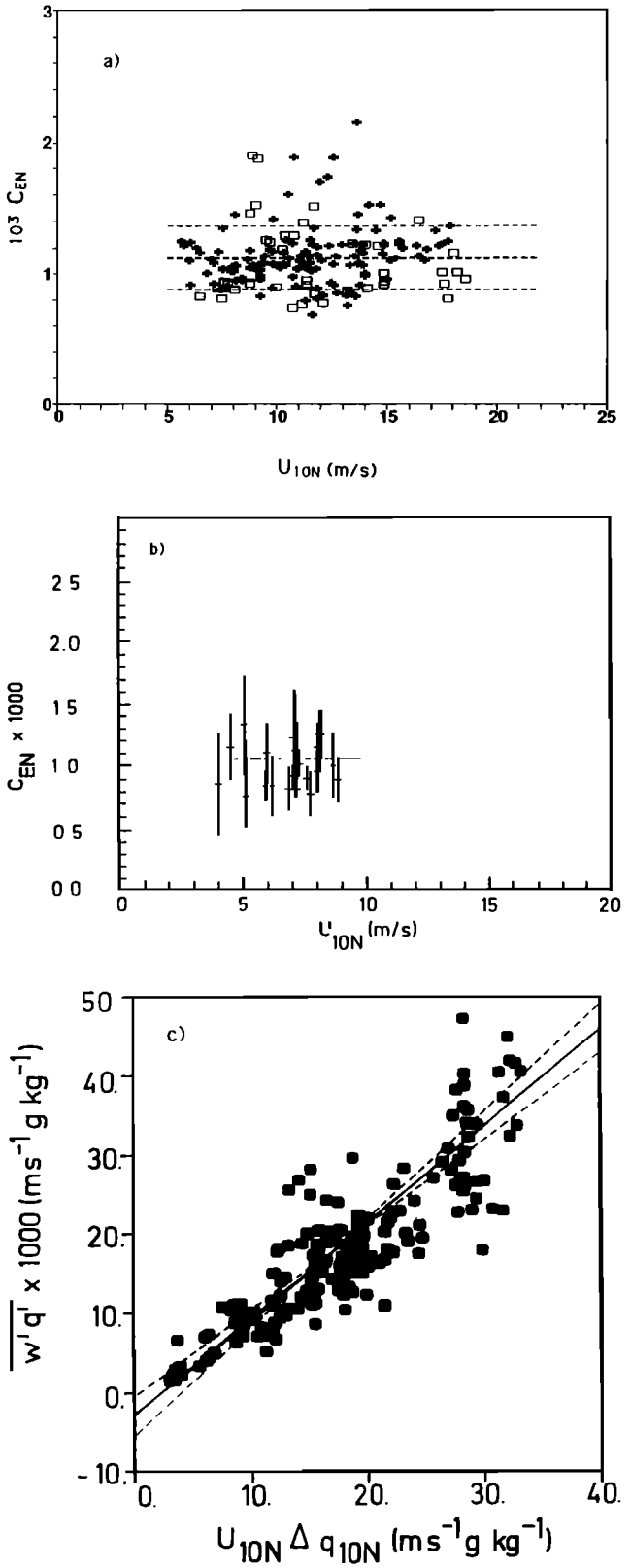

Figure 6. (a) Vapor flux exchange coefficients from UW (crosses) and BIO (squares) data. Thick dashed line is the average value, 1.12×10^{-3} for 170 data points. Thin dashed lines indicate standard deviations. (b) Vapor flux exchange coefficients from IfM tripod data. (c) Measured versus parameterized vapor flux from IfM measurements. Forward and reverse regressions are indicated by dashed lines, average regression is solid line, which has a slope of 1.21.

131 UW data runs and 39 BIO runs, giving an average water vapor flux exchange coefficient adjusted to 10-m height and neutral stratification of

$$C_{EN} = (1.12\pm0.24)\times10^{-3} \quad (14)$$

Contrary to the dramatic predictions from *Bortkovskii's* [1987] or *Ling et al.'s* [1980] sea spray evaporation models, a linear regression analysis on the combined UW and BIO data does not show any significant increase in the water vapor exchange coefficient with increasing wind speed up to 18 m/s. UW data alone show a slight increase with wind speed, while BIO data alone show a weak decrease (both less than 15%, and with low correlation coefficients). The difference between these "best fits" to subsets of the data illustrates the uncertainty of a small dependence of C_{EN} on wind speed (see discussion below).

The IfM water vapor flux results. Figures 6b and 6c show the water vapor flux results derived from the 19 hours of measurements. The average value of C_{EN} derived from these data is $1.05\pm0.22\times10^{-3}$. However, due to detected errors in water temperature associated with tides and insolation, the error in the bulk product $U_{10N}\times(Q_s-Q)$ is comparable to the error in the measured flux. Therefore a better estimate of C_{EN} comes from the average of the two linear regressions shown in Figure 6c, with bulk product and flux taken each in turn as the independent and dependent variable. The slopes of the two regressions are related through the correlation coefficient. The average regression gives a value of C_{EN} of $(1.21\pm0.28)\times10^{-3}$ over the wind speed range 4-10 m/s, which agrees well with the values obtained from MPN. No significant change of the Dalton number with wind speed was seen in these data.

The downward flux seen in Figure 6c at vanishing $U_{10N}\times(Q_s-Q)$ arises from choosing the two-way regression over the one-way regression. It is of marginal significance and may be related to cool skin effects at the air-sea interface [e.g., *Kruspe*, 1977].

The BMO water vapor flux results. A summary of the humidity flux results from flights H760 and H762 at the lowest level (30-40 m) is given in Table 2. The average values of the water vapor flux exchange coefficient for these flights, adjusted to 10-m height and neutral stability, are 0.85×10^{-3} and 1.02×10^{-3}, respectively. These values are 10-32% lower than those obtained on the platform and the tower; however, the aircraft data were filtered with a 1-Hz low-pass filter, and it is estimated that the measured fluxes may be as much as 10% below their actual values due to loss of high-frequency contributions to the covariances. Figures 7a and b show that the water vapor flux was fairly constant throughout the boundary layer for both of the reported cases, indicating vigorous entrainment at the top of the boundary layer. Both flights took place in partly cloudy conditions, with 4–5 oktas of cumulus noted during flight H760 and 1–2 oktas of growing cumulus during flight H762. Observations have shown that growing cumulus clouds are very efficient at removing moisture from the lower atmosphere [*Pennell and LeMone*, 1974].

Sensible Heat Flux Results

Sensible heat flux measurements are difficult to make in the marine surface layer. The problem of salt contamination of the sensors has already been discussed, and despite our efforts to protect the sensors, a significant amount of the data were found to be affected by this phenomenon. The calculation of the sensible heat flux coefficient also depends on the value of the air-sea

Table 2. Water vapor and sensible heat flux results from flights H760 and H762 during HEXMAX

Run	Leg	Start Time	End Time	Height, m	U (30m), m/s	T_{air}, °C	T_{sea}, °C	T_{sea} – MPN, °C	Q_{air}, g/kg	C_{DN10} ×1000	C_{HN10} ×1000	C_{EN10} ×1000	z/L
						Flight H760 (October 22)							
3	CD	1136	1143	37.2	8.54	12.07	13.87	13.8	-	1.17	0.57	-	-0.18
4	CD	1147	1155	40.8	8.35	11.98	13.84		6.39	0.93	0.61	0.88	-0.33
9	CD	1241	1249	32.5	7.85	11.75	13.68	13.8	6.65	1.56	0.69	1.06	-0.16
10	AB	1256	1305	39.9	8.47	12.12	14.30		6.60	1.02	0.58	1.06	-0.30
11	GH	1314	1322	42.9	8.85	12.27	14.41	13.7	6.59	1.22	0.82	1.07	-0.32
16	GH	1406	1413	38.1	9.62	12.29	14.33		6.68	1.54	0.69	1.22	-0.14
						Flight H762 (October 29)							
3	CD	1138	1145	37.2	10.57	10.43	11.95	12.0	4.63	1.17	0.55	0.87	-0.11
6	CD	1213	1222	35.8	10.80	10.51	11.88		4.49	1.12	1.07	1.10	-0.18
9	CD	1250	1256	34.5	10.73	10.62	11.96	12.1	4.47	1.03	0.60	1.05	-0.10
12	AB	1327	1337	36.3	10.49	10.68	12.64		4.49	1.16	0.97	1.18	-0.22
15	GH	1352	1401	38.8	10.95	10.80	13.07	12.1	4.56	1.04	0.99	0.97	-0.30
18	GH	1428	1435	36.2	9.95	10.85	13.11		4.71	1.27	0.69	1.06	-0.19
22	GH	1515	1523	35.5	11.43	11.12	13.11	12.2	4.56	1.34	0.71	0.95	-0.11

temperature difference. When this temperature difference is so small that it approaches the value of the accuracy of the measurements, the percentage error in the exchange coefficient introduced through this term alone may approach 100%. Under these conditions the sensible heat flux will also be very small and difficult to measure accurately. The difference between the bucket and skin temperatures, although small for high wind speeds which prevailed during HEXMAX, may be significant when the air and sea temperatures are within a degree of each other. For the conditions encountered during HEXMAX, the sensible heat flux values are estimated to contain more error than the water vapor fluxes, and fewer data runs were judged to be of high enough quality to use for further analysis.

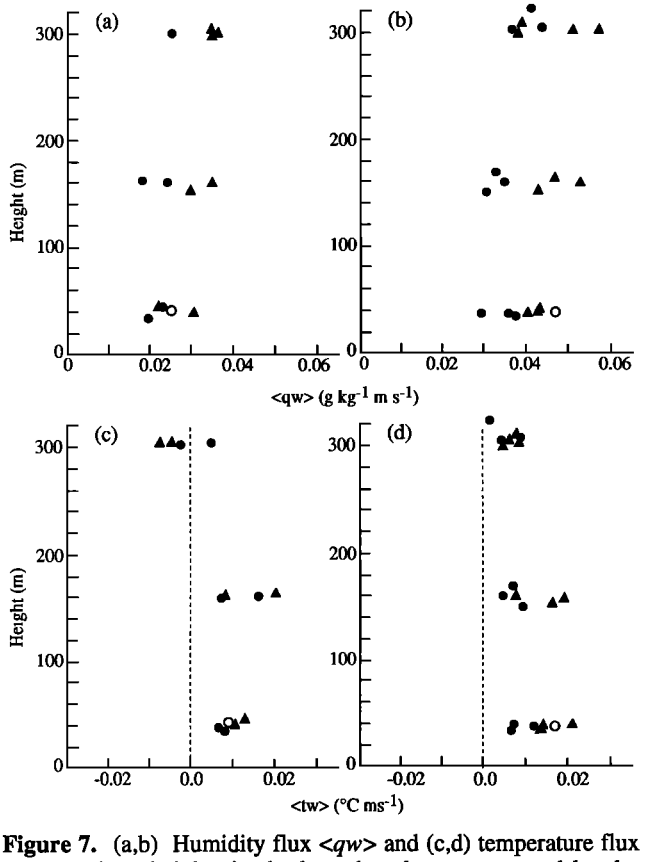

Figure 7. (a,b) Humidity flux <*qw*> and (c,d) temperature flux <*tw*> at three heights in the boundary layer, measured by the BMO aircraft during flights (a and c) H760 and (b and d) H762. (See Table 2 for values at 30 to 40-m height.) Solid circles indicate data collected on leg CD, triangles on leg GH, and open circles on leg AB.

Although the scatter in the data is considerable, the results of the sensible heat flux measurements from the participating groups are in good general agreement. Samples of the cospectra of vertical velocity and temperature are found in Figure 4b. Gradual roll-off of Fastip response is seen above 0.1 Hz. Peaks at 0.4 and 1.0 Hz suggest possible contamination of the microbead thermistor. These problems demonstrate the importance of redundant measurements in these inhospitable conditions. The values of C_{HN} derived from UW and BIO data are shown in Figure 8. The scatter is greater than in the case of the water vapor exchange coefficient, with the standard deviation being closer to 40% even for this subset of the data judged to be of high quality. C_{HN} is constant within experimental uncertainty, the average value derived from 133 runs of UW and BIO HEXMAX data covering a wind speed range of 6–23 m/s being

$$C_{HN} = (1.14 \pm 0.35) \times 10^{-3} \quad (15)$$

This value is 13% higher than has typically been measured over the open ocean for slightly unstable low-level stratification [e.g., *Smith*, 1980, 1988; *Geernaert*, 1990; *Large and Pond*, 1982). A constant value of the sensible heat exchange coefficient for slightly unstable, near-neutral conditions describes the data, on average, very well. No significant dependence of C_{HN} on wind speed is seen in these data.

In the analysis of the UW HEXMAX data, we have limited our sample to those cases with at least a 1.5°C sea-air temperature difference to eliminate large errors in the estimation of the heat flux exchange coefficient (for mean temperatures accurate to ±0.2°C, the temperature difference is accurate to ±0.3°C (rms), which is 20% of the selected minimum difference).

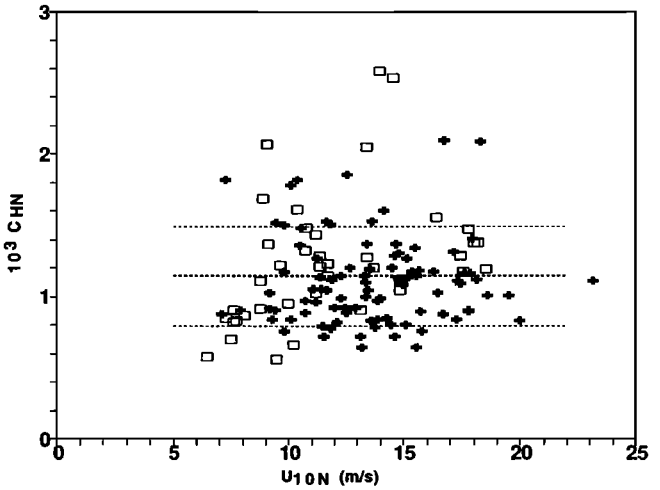

Figure 8. Sensible heat exchange coefficient C_{HN} from UW (crosses) and BIO (squares) data. Thick dashed line is the average value $C_{HN} = 1.14 \times 10^{-3}$ for 133 data points. Thin dashed lines indicate standard deviation.

The BIO temperature measurements were taken with both microbead and Fastip thermistors [*Katsaros et al.*, 1994]. The mean flux coefficient from the Fastip thermistor data, adjusted to 10-m height and neutral stability was $(1.13 \pm 0.26) \times 10^{-3}$ for 30 data runs with air-sea temperature difference exceeding 1°C.

The heat transfer coefficient C_{HN}, derived from the C-130 sensible heat flux data is 30-42% lower than results from the other groups (Table 2). Figures 7c and d show the variation in sensible heat flux with height for flights H760 and H762. Unlike the moisture flux, the sensible heat flux is not constant but decreases with height above the surface layer. The average coefficient found for the slightly unstable conditions during flights H760 and H762 was 0.73×10^{-3}. The skin temperature of the sea was measured from the aircraft with a Barnes PRT-5 radiometer. This measurement must be corrected for non-blackness of the sea surface. The correction varies with cloud cover [*Liu and Katsaros*, 1984]. The difference between the skin and bucket temperatures and the variation of the measured radiative temperature with other parameters such as whitecap coverage are all possible sources of error.

In the bulk formulas, (9) and (10), bucket temperature is often used for T_s and for computation of the saturation humidity at the surface. The skin temperature differs from the bulk temperature due to radiative, sensible, and latent heat fluxes [*Saunders*, 1967; *Kruspe*, 1977]. Differences in the range -0.6° to $+0.7^\circ$C have been measured in the field [e.g., *Ewing and McAlister*, 1960; *Katsaros*, 1977]. For legs CD on flights H760 (October 22, 1986) and H762 (October 29), the bulk temperatures at MPN were equal to the skin temperatures (Table 2) within 0.1°C.

Discussion

The heat and humidity flux coefficients (9) and (10) would be constant (after adjustments to neutral stability and standard 10-m reference height) if the surface fluxes were simply proportional to bulk differences and to wind speed. Therefore, other physical processes that affect the surface fluxes must result in variation of these coefficients. No significant variation of these coefficients with wind speed has been found.

Combining the bulk formulas (8)-(10) with the surface-layer profiles for neutral density stratification, (1)-(3), the neutral exchange coefficients may be expressed in terms of the roughness lengths for wind speed, temperature, and water vapor, z_0, z_t, and z_q

$$C_{DN} = \frac{k^2}{\ln\left(z/z_0\right)^2} \tag{16}$$

$$C_{HN} = \frac{k^2}{\left[\ln\left(z/z_0\right)\ln\left(z/z_t\right)\right]} = C_{DN}^{1/2}\frac{k}{\left[\ln\left(z/z_t\right)\right]} \tag{17}$$

$$C_{EN} = \frac{k^2}{\left[\ln\left(z/z_0\right)\ln\left(z/z_q\right)\right]} = C_{DN}^{1/2}\frac{k}{\ln\left(z/z_q\right)} \tag{18}$$

The neutral coefficients are used to compare fluxes measured in different wind speed and stratification conditions. If z_t and z_q were independent of z_0, then from (17) and (18), C_{EN} and C_{HN} would be expected to vary with $C_{DN}^{1/2}$; Launiaien [1983] suggested a linear dependence on C_{DN}. In Figure 9a it is clear that the evaporation coefficient and the square root of the drag coefficient are indeed correlated. A regression line

$$10^3 C_{EN} = 1.26(10^3 C_{DN})^{1/2} - 0.49 \tag{19}$$

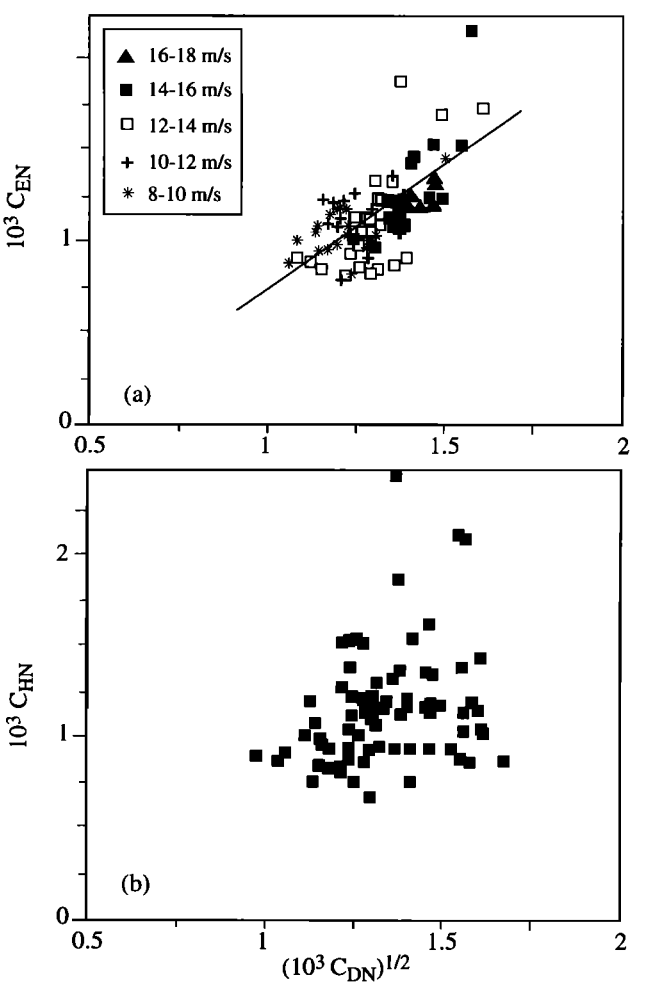

Figure 9. (a) C_{EN} and (b) C_{HN} versus square root of drag coefficient, UW data only. (a) Symbols in indicate wind speed categories in 2 m/s ranges, and regression line is (19).

gives a correlation coefficient of 0.63 for 98 points. A Student's t-test indicates that this relationship is highly significant. Similar variation of C_{HN} with $C_{DN}^{1/2}$ is hypothesized, although Figure 9b shows that the scatter in these data prohibits drawing any conclusions.

The symbols in Figure 9a sort th data by wind speed in 2 m/s categories, and within each category the points follow a similar relation, i.e., for a given wind speed, C_{EN} increases with increasing $C_{DN}^{1/2}$. Figure 10 helps to elucidate this point: there is much variation of C_{DN} in these data for a given wind speed, and it is this variation of the drag coefficient that correlates with the variation in C_{EN}. This so-called scatter (larger than experimental error) has been observed in all attempts to measure the surface fluxes (see the review paper by *Donelan* [1990] for a discussion of this point) and is considered to be an indication of the dependence of sea surface drag on processes operative in the marine surface layer that are not completely understood. Recent studies, including analysis of the HEXOS data [*Smith et al.*, 1992; *Donelan et al.*, 1993] for example, have found some of the variation of C_{DN} at a given wind speed to be due to variation in sea state: "young" seas in which waves at the peak of their spectrum travel significantly slower than the wind are rougher (higher z_0 and C_{DN}) than "mature" waves traveling at approximately the wind velocity. (Because C_{DN} increases with wind speed and C_{EN} does not, the lower wind speed categories (asterisk and cross symbols in Figure 9a) tend to lie to the left of the regression line (19), and the higher speed categories (solid symbols in Figure 9a) to the right.) These results may indicate that the water vapor flux is also correlated with wave age, though there are not enough data here to verify that relationship directly. The influence on the correlation in Figure 9a of the mean wind speed as a common parameter in both exchange coefficients has been investigated. Elimination of this common factor yields an even stronger correlation, so we can be certain that the relationship (19) is not spurious.

To maintain a nearly constant C_{EN} over the entire wind speed range, z_q and z_t must decrease with increasing wind speed. The roughness lengths, z_0, z_t, and z_q, (16)–(18), are exponential functions of the exchange coefficients; because of the large variability of individual values, they are grouped for this analysis in wind speed ranges of 2 m/s. Due to this variability, the median values of z_0, z_t, and z_q (Figure 11) are more representative of each category than are the means (also shown). Interquartile ranges indicate the amount of scatter in the data. Figure 11a illustrates that z_q decreases with increasing wind speed. Except for the highest (>17 m/s) wind speed category, this trend closely follows the predictions of *Liu et al.* [1979] (henceforth *LKB*) as implemented in the UW boundary layer model [*Brown and Liu*, 1982].

This variation in z_q implies that the ratio of q_* to the low level humidity gradient decreases with increasing winds, even as the ratio of u_* to U_{10} increases. The latter is an indication of an increase in mechanical turbulence. Thus there seems to be a

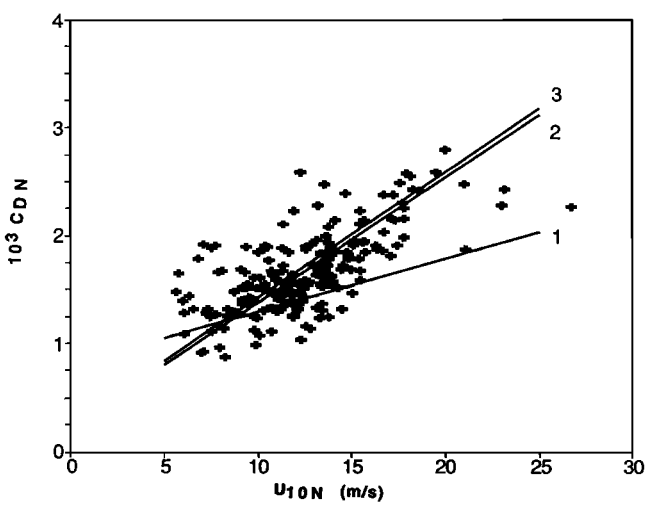

Figure 10. The drag coefficient C_{DN}, versus U_{10N}. Line 1 [*Smith*, 1988] indicates typical open-ocean results; line 2 [*Smith et al.*, 1992] is combined HEXOS line $10^3 C_{DN} = 0.27 + 0.116 U_{10N}$ from data using K-Gill, pressure, and sonic anemometers; and line 3 is regression fitted to just the UW data [*DeCosmo*, 1991].

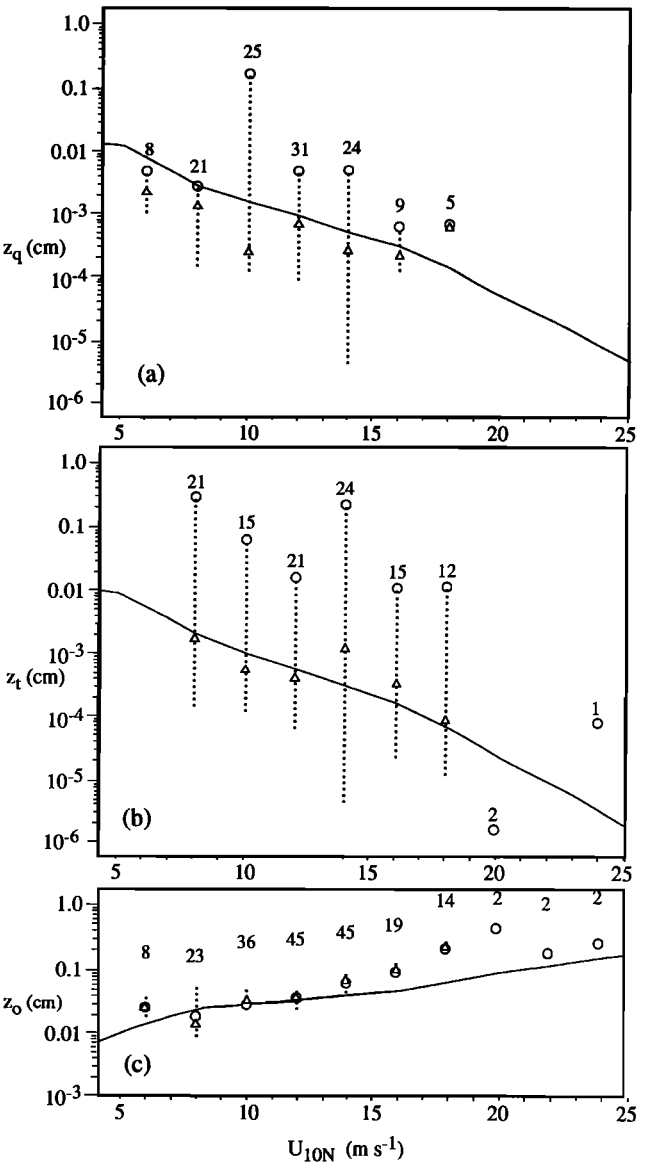

Figure 11. Log of (a) water vapor roughness length z_q, (b) temperature roughness length z_t, and (c) roughness length z_o for the UW data and as predicted by *Liu et al.* [1979] using the model of *Brown and Liu* [1982] (solid lines). Data have been combined in 2 m/s wind speed categories. Within each category, triangles represent the median value, dotted lines the interquartile range, and circles the mean; the number of points in each category is shown.

mechanism relevant to the scalar fluxes that inhibits the increase of the exchange of scalar quantities and counteracts any increased flux that would be due to enhanced mechanical mixing close to the air-sea interface in moderately strong winds. The LKB model behavior was explained by the process of sheltering in the wave troughs. This process may become more important as the waves grow larger. On the other hand, no effects of wave breaking were considered in that model. Others [e.g., *Donelan*, 1990; *DeCosmo*, 1991] have postulated that, at wind speeds above 7–10 m/s, the decrease due to sheltering may be offset by other processes such as the disruption of the surface microlayer by breaking waves.

The median values of z_t for 2 m/s wind speed categories also follow closely the prediction of the LKB model (Figure 11b). Because of the larger scatter in z_t, the conclusion that it behaves in the same way as z_q is tentative until corroborated by other data sets.

Values of z_0 (Figure 11c) are numerically much larger than those of z_q or z_t. They follow the model of LKB only up to a wind speed of 12 m/s. At higher wind speeds, there is an increase in z_0 that *Smith et al.* [1992] have attributed to form drag on choppy "young" waves traveling slower than the wind. This situation typically occurs during periods of high winds at the coastal MPN site when the long waves interact with the sea bottom. This phenomenon is well documented, and its effect on wind stress has been observed in several other studies at shallow sites [e.g., *Donelan*, 1982; *Geernaert et al.*, 1986].

Over the wind speed range 6–18 m/s the observed increase in z_0 implies an increase of about 25% in C_{EN}; the observed decrease in z_q implies a decrease of about 15% in C_{EN}. A net increase of 10% remains, which is no larger than the estimated accuracy of the measurements. The UW data alone show an increase of the order of 10% over the wind speed range 6–18 m/s, with no statistical significance; on the other hand, the BIO data taken alone show a similar decrease, also with a very small correlation coefficient. Rather than indicating that over the entire data set there is no net increase or decrease of C_{EN} with wind speed, these measurements may suggest that the 1.4-m vertical distance between the instrument packages was critical to the flux measurements. The lower (BIO) package may have been exposed to more liquid droplets and less vapor flux, while the higher instruments saw a greater percentage of the overall effect on fluxes. Clearly, the lack of statistical significance and the magnitude of experimental error prohibit any firm conclusions. Measurements at heights within and above the spray layer are needed to sort out these effects.

The above interpretation is based on calculation of the roughness lengths from (16)–(18), which assumes logarithmic forms for the profiles (1)–(3). If the evaporation of spray droplets in layers below the measuring height altered the shapes of the temperature and humidity profiles, then the roughness lengths derived from the fluxes would not be correct, and the above interpretation would have to be modified. All of our results indicate much less influence of spray than had been anticipated, and so we have confidence in the above interpretation.

These results lead to three hypotheses: (1) the flux of water by evaporation of droplets is too small to have an overall measurable effect in the range of observation, (2) compensating effects take place between the surface and the measuring height that reduce the net influence of evaporating droplets to a level that we cannot detect, or (3) the droplet evaporation layer may have extended above the measurement level, so that some portion of the source of water vapor from evaporating droplets was not included in these measurements. Compensating effects may include negative feedback by the heat and moisture flux from the sea spray on the low-level humidity and temperature profiles, partially inhibiting the turbulent fluxes from the surface [*Katsaros and DeCosmo*, 1990; *DeCosmo*, 1991; *Andreas et al.*, 1995]. Direct measurements of the source of spray droplets and of the profiles of temperature and humidity in the layer just above the interface will be needed to distinguish between these hypotheses.

Conclusions

1. Protection of humidity and temperature eddy-flux sensors with aspirated shields [*Katsaros et al.*, 1994] has made it possible to obtain high-quality measurements of water vapor and sensible heat fluxes over the sea in conditions where in past attempts, salt spray has damaged the sensors.

2. The HEXOS water vapor and sensible heat flux measurements, adjusted to neutral stratification and 10-m height, may be summarized by

$$C_{EN} = C_{HN} = 1.1\times10^{-3} \tag{20}$$

and no significant variation with wind speed has been found for wind speeds up to 18 m/s for C_{EN} and up to 23 m/s for C_{HN}. Within experimental uncertainty, these do not differ significantly from reviews of existing data, $C_{EN} = 1.2\times10^{-3}$ [*Smith*, 1989] and $C_{HN} = 1.0\times10^{-3}$ [*Smith*, 1988].

3. An increase of C_{EN} by as much as 20%, or even a small decrease in C_{EN} over the wind speed range 5–18 m/s, is not ruled out, but a sudden and dramatic increase of C_{EN} due to evaporation of spray droplets, predicted by several models at wind speeds beyond about 15 m/s, has not been found in these data. Scatter in the values of C_{HN} precludes reaching firm conclusions, but apart from its scatter, it does not seem to differ from C_{EN}.

4. The evaporation coefficient is correlated with the square root of the drag coefficient, even though C_{EN} does not mirror the latter's wind speed dependence. This indicates that other processes that influence C_{DN} and the surface roughness z_0 (at a given wind speed), notably sea state, may also influence C_{EN}.

5. The nonlinear increase in u_* with wind speed (i.e., the increase of C_{DN} and z_0 with wind speed) is not accompanied by an increase in C_{EN} (C_{HN} behaves similarly, but there is more scatter in those data). Consequently, z_q (and z_t) must decrease with increasing wind speed. This decrease may be due to sheltering in the wave troughs, as postulated by LKB. This theory was not intended to apply for wind speeds higher than about 7–10 m/s because it does not take into account the influence of breaking waves. However, Figure 11 shows that it is in agreement with HEXMAX vapor flux data for wind speeds up to 16 m/s and HEXMAX heat fluxes up to 18 m/s. This agreement does not prove the validity of the physics used to derive the LKB model. It does indicate that predictions of water vapor and sensible heat flux using this model are in accord with measurements up to moderately high winds. Unlike the vapor and sensible heat flux coefficients, the drag coefficient at MPN increases more rapidly than at deep water sites or than the prediction of LKB. In applying the LKB model, either an adjustment of wind stress for wave age or a site-specific adjustment of wind stress at shallow coastal sites is indicated.

Measurements of water vapor flux at up to 18 m/s were a significant technological achievement, leading to advances in

understanding and modeling. We still do not know if evaporation of spray causes rapid increases in C_{EN} at yet higher wind speeds. Experiments designed to explore even stormier conditions will become progressively more difficult. Eddy fluxes should be measured at higher levels, perhaps about 20 m, to remain above most of the spray layer, and further refinement of protective shields or more robust fast humidity sensors will be needed. A site in deeper water will be needed because the waves will be higher, longer, faster, and deeper. There remains an urgent need to measure the source function of spray droplets in these extreme conditions.

Acknowledgments. The authors wish to thank C. Kraan, J. Schaap, C. van Oort and E. Worrell of KNMI; R. Foster, S.S. Ataktürk and R.J. Lind of UW; D.L. Hendsbee of BIO; and H. Fechner, P.R. Timm, and K. Uhlig of IfM. We are also indebted to an anonymous reviewer, who provided important suggestions about an interpretation of the differences between the UW and BIO water vapor flux data. The two lead authors were funded by the Office of Naval Research under grant N00014-85-K-0123, and by the National Science Foundation under grant ATM-9024698. Participation of IfM was funded by Deutsche Forschungsgemeinschaft, SFB 133, "Warmwassersphare des Nordatlantiks." HEXOS contribution 42.

References

Anderson, R.J., and S.D. Smith, Evaporation coefficient for the sea surface from eddy flux measurements, *J. Geophys. Res.*, 86, 449-456, 1981.

Andreas, E.L., Sea spray and the turbulent air-sea heat fluxes. *J. Geophys. Res., 97,* 11,429-11,441, 1992.

Andreas, E.L., Reply to "Comment on 'Sea spray and the turbulent air-sea heat fluxes'by E.L. Andreas" by K.B. Katsaros and G. de Leeuw. *J. Geophys. Res., 99*, 14,345-14,350, 1994.

Andreas, E.L, J.B. Edson, E.C. Monahan, M.P. Rouault, and S.D. Smith, The spray contribution to net evaporation from the sea: A review of recent progress, *Boundary Layer Meteorol., 72*, 3-52, 1995.

Ataktürk, S.S., and K.B. Katsaros, The K-Gill: A twin propeller-vane anemometer for measurements of atmospheric turbulence., *J. Atmos. Oceanic Technol.,* 6, 509-515, 1989.

Behrens, K., *Turbulente wind fluktuationen und verticale fluesse im Kuestenvorfeld*, Berl *233*, 81 pp., Inst. fuer Meereskunde an der Christian-Albrechts-Univ. Kiel, 1993.

Bortkovskii, R.S., *Air-Sea Exchange of Heat and Moisture During Storms,* xii + 194 pp., D. Reidel, Norwell, Mass., 1987.

Brown, R.A., and W.T. Liu, An operational large-scale marine planetary boundary layer model, *J. Appl. Meteorol., 21*, 261-269, 1982.

Brutsaert, W., A theory for local evaporation (or heat transfer) from rough and smooth surfaces at ground level, *Water Resour. Res., 11*, 543-550, 1975.

Busch, N.E., On the mechanics of atmospheric turbulence, in *Workshop on Micrometeorology,* edited by D.A. Haugen, pp. 1-65, Am. Meteorol. Soc., Boston, Mass., 1973.

Businger, J.A., Equations and concepts, in *Atmospheric Turbulence and Air Pollution Modeling,* edited by F.T.M. Nieuwstadt and H. van Dop, pp. 1-36, D. Reidel, Norwell, Mass., 1982.

Businger, J.A., J.C. Wyngaard, Y.K. Izumi, and E.F. Bradley, Flux-profile relations in the atmospheric surface layer, *J. Atmos. Sci., 28*, 181-189, 1971.

Davidson, K.L., T.M. Houlihan, C.W. Fairall, and G.E. Schacher, Observation of the temperature structure function parameter, C_T^2 , over the ocean. *Boundary Layer Meteorol., 15*, 507-523, 1978.

Deacon, E.L., Gas transfer to and across an air-water interface, *Tellus, 29*, 363-375, 1977.

DeCosmo, J., *Air-sea exchange of momentum, heat, and water vapor over whitecap sea states.* Ph.D. thesis, 212 pp., Dep. of Atmos. Sci., Univ. of Wash., Seattle, May, 1991. pp. 212. (Available from University Microfilms, 300 North Zeeb Road, Ann Arbor, Mich., 48106.)

Donelan, M.A., The dependence of the aerodynamic drag coefficient on wave parameters, in *First International Conference on Meteorology and Air-Sea Interaction of the Coastal Zone,* pp. 381-387, Amer. Meteorol. Soc., Boston, Mass., 1982.

Donelan, M.A., Air-sea interaction, in *The Sea: Ocean Engineering Science,* vol. 9., edited by B. LeMehaute and D. Hanes, pp. 239-292, John Wiley, New York, 1990.

Donelan, M.A., F.W. Dobson, S.D. Smith, and R.J. Anderson, On the dependence of sea-surface roughness on wave development, *J. Phys. Oceanog., 23*, 2143-2149, 1993.

Dyer, A.J., A review of flux-profile relationships. *Boundary Layer Meteorol., 7*, 363-372, 1974.

Edson, J.B., Lagrangian model simulations of the turbulent transport of evaporating jet droplets, Ph.D. thesis, 141 pp., Dep. of Meteorol., Penn. State Univ., University Park, 1989.

Edson, J.B., C.W. Fairall, P.G. Mestayer, and S.E. Larsen, A study of the inertial-dissipation method for computing air-sea fluxes, *J. Geophys. Res., 96*, 10,689-10,711, 1991.

Ewing, G., and E.D. McAlister, On the thermal boundary layer of the ocean, *Science, 13*, 1374-1376, 1960.

Fairall, C.W., K.L. Davidson, and G.E. Schacher, Humidity effects and sea salt contamination of atmospheric temperature sensors, *J. Appl. Meteorol., 18*, 1233-1239, 1979.

Fairall, C.W., K.L. Davidson, and G.E. Schacher, An analysis of the surface production of sea-salt aerosols, *Tellus, Ser.B, 35*, 31-39, 1983.

Fairall, C.W., J.B. Edson, S.E. Larsen, and P.G. Mestayer, Inertial dissipation of air-sea flux measurements: A prototype system using real time spectral computations, *J. Atmos. Oceanic Technol., 7*, 425-453, 1990.

Fleagle, R.G., and J.A. Businger, *An Introduction to Atmospheric Physics*, 2nd ed., 432 pp., Academic , San Diego, Calif., 1980.

Friehe, C.A., and K.B. Schmitt, Parameterization of air-sea interface fluxes of sensible heat and moisture by the bulk aerodynamic formulas, *J. Phys. Oceanogr., 6*, 801-809, 1976.

Garratt, J.R., and P. Hyson, Vertical fluxes of momentum, sensible heat and water vapor during the Air Mass Transformation Experiment (AMTEX) 1974, *J. Meteorol. Soc. Jpn., 53*, 149-160, 1975.

Geernaert, G.L., Bulk parameterizations for the wind stress and heat fluxes, in *Surface Waves and Fluxes,* edited by G.L. Geernaert and W.J. Plant, pp. 91-172, Kluwer, Dordrecht, the Netherlands, 1990.

Geernaert, G.L., K.B. Katsaros, and K. Richter, Variation of the drag coefficient and its dependence on sea state, *J. Geophys. Res., 91*, 7667-7679, 1986.

Isemer, H.J. and L. Hasse, *The BUNKER Climate Atlas of the North Atlantic Ocean,* vol. 2, *Air-Sea Interactions*, 256 pp., Springer-Verlag, New York, 1987.

Isemer, H.J., J. Willebrand, and L. Hasse, Fine adjustments of large scale air-sea energy flux parameterizations by direct estimates of ocean heat transport, *J. Clim., 2*, 1173-1184, 1989.

Katsaros, K.B., The sea surface temperature deviation at very low wind speeds: Is there a limit? *Tellus, 29*, 229-239, 1977.

Katsaros, K.B., and J. DeCosmo, Evaporation at high wind speeds, sea surface temperature at low wind speeds: Examples of atmospheric regulation, in *Modeling the Fate and Influence of Marine Spray,* Whitecap Rep. 7, edited by P.G. Mestayer, E..C. Monahan and P.A. Beetham, pp. 106-114, Mar. Sci. Inst., Univ. of Conn., Avery Point, Groton, 1990.

Katsaros, K.B., and G. de Leeuw, Comment on "Sea spray and the turbulent air-sea heat fluxes" by Edgar L. Andreas, *J. Geophys. Res., 97*, 14,339-14,343, 1994.

Katsaros, K.B., S.D. Smith, and W.A. Oost, 1987: HEXOS - Humidity Exchange Over the Sea: A program for research on water vapor and droplet fluxes from sea to air at moderate and high wind speeds. *Bull. Amer. Meteor. Soc.,* **68**, 466-476.

Katsaros, K.B., J. DeCosmo, R.J. Anderson, S.D. Smith, C. Kraan, W.A. Oost, L. Hasse, K. Bumke, P.G. Mestayer, and M.H. Smith, Measurements of humidity and temperature in the marine environment during the HEXOS Main Experiment, *J. Atmos. Oceanic Technol., 11*, 964-981, 1994.

Kitaigorodskii, S.A., On the fluid dynamical theory of turbulent gas transfer across an air-water interface in the presence of breaking wind-waves, *J. Phys. Oceanogr., 13*, 816-827, 1984.

Kitaigorodskii, S.A. and M.A. Donelan, Wind-wave effects on gas transfer., in *Gas Transfer at Air-Water Surface,* edited by W. Brutsaert and Jirka, pp. 147-170, D. Reidel, Norwell, Mass., 1984.

Kruspe, G., On moisture-flux parameterization, *Boundary Layer Meteorol., 11*, 55-63, 1977.

Large, W.G., and S. Pond, Sensible and latent heat flux measurements over the ocean, *J. Phys. Oceanogr., 12*, 464-482, 1982.

Launiainen, J., Parameterization of the water vapour flux over a water

surface by the bulk aerodynamic method, *Ann. Geophys., 1*, 481-492, 1983.

Ling, S.C., and T.W. Kao, Parameterization of the moisture and heat transfer processes over the ocean under whitecap sea states, *J. Phys. Oceanogr., 6*, 306-315, 1976.

Ling, S.C., A. Saad, and T.W. Kao, Mechanics of multi-phase fluxes over the ocean, in *Turbulent Fluxes Through the Sea Surface, Wave Dynamics, and Prediction*, edited by A. Favre and K. Hasselmann, pp. 185-197, Plenum, New York, 1978.

Ling, S.C., T.W. Kao, M. Asce, and A. Saad, Microdroplets and transport of moisture from the ocean. *J. Eng. Mech. Div., Am. Soc. Civ. Eng., 6*, 1327-1339, 1980.

Liu, W. T., and K. B. Katsaros, Analysis of sea surface, air temperature and turbulence fluxes measured from aircraft in Joint Air Sea Interaction (JASIN) experiment., *J. Geophys. Res., 89*, 10,641-10,644, 1984.*9*,

Liu, W.T., K.B. Katsaros, and J.A. Businger, Bulk parameterization of air-sea exchanges of heat and water vapor, including the molecular constraints at the interface, *J. Atmos. Sci., 36*, 1722-1735, 1979.

Merlivat, L., The dependence of bulk evaporation coefficients on air-water interfacial conditions as determined by the isotopic method, *J. Geophys. Res., 83*, 2977-2980, 1978.

Mestayer, P.G., and C. Lefauconnier, Spray droplet generation, transport and evaporation in tunnel during HEXIST (HEXOS experiments in the simulation tunnel), *J. Geophys. Res., 93*, 572-586, 1988.

Mestayer, P.G., et al., CLUSE simulations of the vapor flux modification by droplet evaporation, in *Modeling the Fate and Influence of Marine Spray,* Whitecap Rep. 7, edited by P.G. Mestayer, E.C. Monahan, and P.A. Beetham, pp. 100-105, Mar. Sci. Inst., Univ. of Conn., Avery Point, Groton, Conn., 1990a.

Mestayer, P.G., E.C. Monahan, and P.A. Beetham (Eds.), *Modelling the Fate and Influence of Marine Spray: Proceedings of a Workshop Held 6-8 June 1990, Luminy, France,* Whitecap Rep. 7, Mar. Sci. Inst., Univ. of Conn., Avery Point, Groton, Conn., 1990b.

Monahan, E.C., and I. O'Muircheartaigh, Optimal power-law description of oceanic whitecap coverage dependence on wind speed, *J. Phys. Oceanogr., 10*, 2094-2099, 1980.

Monahan, E.C., C.W. Fairall, K.L. Davidson, and P.J. Boyle, Observed interrelations between 10 m winds, ocean whitecaps and marine aerosols, *Q. J. R. Meteorol. Soc., 109*, 379-392, 1983a.

Monahan, E.C., D.E. Spiel, and K.L. Davidson, Model of marine aerosol generation via whitecaps and wave disruption, in *AMS Preprint Volume of Extended Abstracts: Ninth Conference on Aerospace and Aeronautical Meteorology,* Am. Meteorol. Soc., Boston, Mass., 1983b.

Monahan, E.C., D.E. Spiel, and K.L. Davidson, A model of marine aerosol generation via whitecaps and wave disruption. In *Oceanic Whitecaps and Their Role in Air-Sea Exchange Processes,* edited by E.C. Monahan and G. MacNiocaill, pp. 167-174, D. Reidel, Norwell, Mass., 1986.

Nicholls, S., Measurements of turbulence in an instrumented air-craft in a convective atmospheric boundary layer over the sea, *Q. J. R. Meteorol. Soc., 104*, 653-676, 1978.

Oost, W.A., The pressure anemometer-An instrument for adverse circumstances, *J. Clim. Appl. Meteorol., 22*, 2075-2084, 1983.

Oost, W.A., E.H.W. Worrell, J.W. Schaap, C. van Oort, and C. Kraan, An improved version of the pressure anemometer, *J. Atmos. Oceanic Technol., 8*, 575-584, 1991.

Oost, W.A., C.W. Fairall, J.B. Edson, S.D. Smith, R.J. Anderson, J.A.B. Wills, K.B. Katsaros, and J. DeCosmo, Flow distortion calculations and their application in HEXMAX, *J. Atmos. Oceanic Technol., 11*, 357-365, 1994.

Owen, P.R., and W.R. Thompson, Heat transfer across rough surfaces, *J. Fluid Mech., 15*, 321-334, 1963.

Pennell, W.T. and M.A. LeMone, An experimental study of the turbulence structure in the fair weather trade wind boundary layer, *J. Atmos. Sci., 31*, 1308-1323, 1974.

Preobrazhenskii, L.Y., Estimation of the content of spray-drops in the near-water layer of the atmosphere, *Fluid Mech. Sov. Res., 2*, 95-100, 1973.

Rouault, M.P., Modélisation numérique d'une couche limite unidimensionelle stationnaire d'embruns, Thèse de Doctorat, Univ. d'Aix-Marseille II, France, 1989.

Rouault, M.P., P.G. Mestayer, and R. Schiestel, A model of evaporating spray droplet dispersion, *J. Geophys. Res., 96*, 7181-7200, 1991.

Saunders, P.M., The temperature at the ocean-air interface, *J. Atmos. Sci., 24*, 269-273, 1967.

Schmitt, K.F., C.A. Friehe, and C.H. Gibson, Humidity sensitivity of atmospheric temperature sensors by salt contamination, *J. Phys. Oceanogr., 8*, 151-161, 1978.

Shaw, W.J. and J.E. Tillman, The effect of and correction for different wet-bulb and dry-bulb response in thermocouple psychrometry, *J. Appl. Meteorol., 19*, 90-97, 1980.

Smith, S.D., Eddy flux measurements over Lake Ontario, *Boundary Layer Meteorol., 6*, 235-255, 1974.

Smith, S.D., Wind stress and heat flux over the ocean in gale force winds, *J. Phys. Oceanogr., 10*, 709-726, 1980.

Smith, S.D., Coefficients for sea surface wind stress, heat flux and wind profiles as a function of wind speed and temperature, *J. Geophys. Res., 93*, 15,467-15,472, 1988.

Smith, S.D., Water vapor flux at the sea surface (Review paper), *Boundary Layer Meteorol., 47*, 277-293, 1989.

Smith, S.D., Influence of droplet evaporation on HEXOS humidity and temperature profiles, in *Modeling the Fate and Influence of Marine Spray,* Whitecap Rep. 7, edited by P.G. Mestayer, E.C. Monahan, and P.A. Beetham, pp. 171-174, Mar. Sci. Inst., Univ. of Conn., Avery Point, Groton, Conn., 1990.

Smith, S.D., K.B. Katsaros, W.B. Oost, and P.G. Mestayer, Two major experiments in the Humidity Exchange Over the Sea (HEXOS) program, *Bull. Am. Meteorol. Soc., 71*, 161-172, 1989.

Smith, S.D., R.J. Anderson, W.A. Oost, C. Kraan, N. Maat, J. DeCosmo, K.B. Katsaros, K. Bumke, L. Hasse, and H.M. Chadwick, Sea surface wind stress and drag coefficients: the HEXOS results, *Boundary Layer Meteorol., 60*, 109-142, 1992.

Spillane, M.C., E.C. Monahan, P.A. Bowyer, D.M. Doyle, and P.J. Stabeno, Whitecaps and global fluxes, in *Oceanic Whitecaps and Their Role in Air-Sea Exchange Processes,* edited by E.C. Monahan and G. MacNiocaill, pp. 209-218, D. Reidel, Norwell, Mass., 1986.

Stramska, M., Vertical profiles of sea salt aerosol in the atmospheric surface layer: A numerical model, *Acta Geophys. Polonica, 35*, 87-99, 1987.

Taylor P.K., K.B. Katsaros, J. DeCosmo, H.T. Mengelkamp, S.D. Smith, and R. Kraan, HEXMAX budgets of water vapour and heat exchange at the sea surface, paper presented at the Fifth Conference on Coastal Meteorology, Am. Meteorol. Soc., Miami, Fla., May 6-10, 1991.

Tsukamoto, O., Dynamic response of the fine wire psychrometer for direct measurement of water vapor flux, *J. Atmos. Oceanic Technol., 3*, 453-461, 1986.

Wang, C.S., and R.L. Street, Transfers across an air-water interface at high wind speeds: The effect of spray, *J. Geophys. Res., 83*, 2959-2969, 1978.

Wills, J.A.B., HEXOS model tests on the Noordwijk tower, Rep. R184, 56 pp., Bri. Maritime Technol. Ltd, Teddington, England, 1984.

Wyngaard, J.C., The effects of probe-induced flow distortion on atmospheric turbulence measurements, *J. Appl. Meteorol., 20*, 784-794, 1981.

Wyngaard, J.C., The effects of probe-induced flow distortion on atmospheric turbulence measurements: Extension to scalars, *J. Atmos. Sci., 45*, 3400-3412, 1988.

Zhang, S.F., S.P. Oncley, and J.A. Businger, A critical evaluation of the von Karman constant from a new atmospheric surface layer experiment, paper presented at the *Eighth Symposium on Turbulence and Diffusion,* Am. Meteor. Soc., San Diego, April 26-29, 1988.

R.J. Anderson and S.D. Smith, Department of Fisheries and Oceans, Bedford Institute of Oceanography, P.O. Box 1006, Dartmouth, N.S. B2Y 4A2, Canada. (e-mail: STU_SMITH@bionet.bio.dfo.ca)

K. Bumke, Institut für Meereskunde and der Universitat Kiel, Dusternbrooker Weg 20, D-24105 Kiel, West Germany. (e-mail: kbumke@meereskunde.uni-kiel.d400.de)

H. Chadwick, U.K. Meteorological Office, London Road, Bracknell, Berkshire RG12 2SZ, U.K.

J. DeCosmo, University of Washington, Geophysics Program Box 351650, Seattle, WA 98195-1650, (e-mail: janice@geophys.washington.edu)

K.B. Katsaros, University of Washington, Department of Atmospheric Sciences Box 351640, Seattle, WA 98195-1650 (e-mail: katsaros@atmos.washington.edu)

W.A. Oost, inistry of Transport and Public Works, Royal Netherlands Meteorological Institute, P.O. Box 201, 3730 AE de Bilt, The Netherlands. (email: oost@knmi.nl)

(Received January 1, 1994; revised October 12, 1995; accepted October 31, 1995.)